FUDMA Journal of Sciences (FJS)
ISSN online: 2616-1370
ISSN print: 2645 - 2944
Vol. 10 No. 24, December, 2026, pp 351 – 370
DOI: https://doi.org/10.33003/fjs-2026-1024-6536

Development and Characterization of Modified Starches from Selected Tropical Crops for Potential Application as Sustainable Corrosion Inhibitors

***[1]Rosemary Bassey Awoyale, [1]Ezekiel Adewole, [1]Oluwafemi Temitayo Ogunmodede, [1]Funmilayo Deborah Adewumi, [1]Abiodun Ayodele Ojo, [1]Omolara Abosede Peters and [2]Adeolu Abiodun Awoyale**

[1]Department of Chemical Sciences, Afe Babalola University, Ado- Ekiti, Ekiti State, Nigeria.
[2]Petroleum and Natural Gas Processing Department, Petroleum Training Institute, Effurun, Delta State, Nigeria.

*Corresponding authors' email: rosypolly2017@gmail.com

Received: 05 Aug. 2026
Accepted: 15 Nov. 2026
Published: 18 Nov. 2026

ABSTRACT
The chemical modification of starch offers opportunities to develop renewable biopolymers for industrial applications, including corrosion protection. This study investigated the effects of hydroxypropylation, phosphate cross-linking, and sequential dual modification on the physicochemical, functional, and structural properties of starches isolated from tigernut (Cyperus esculentus), water yam (Dioscorea alata), and trifoliate yam (Dioscorea dumetorum). The starches were characterized using proximate analysis, functional property assessment, Rapid Visco Analysis (RVA), Fourier-transform infrared spectroscopy (FTIR), X-ray diffraction (XRD), scanning electron microscopy coupled with energy-dispersive X-ray spectroscopy (SEM–EDS), and differential scanning calorimetry (DSC). Chemical modification significantly ($p < 0.05$) affected starch properties. Cross-linked starches exhibited lower moisture contents (12.12–12.43%) and higher apparent amylose contents (up to 29.45%) than their hydroxypropylated counterparts. FTIR analysis indicated chemical changes associated with modification while confirming retention of the starch backbone. XRD patterns showed preservation of the native crystalline polymorphs, with relative crystallinity ranging from 23.1 to 33.9%. SEM observations revealed changes in granule morphology, including increased aggregation following cross-linking and dual modification, while EDS detected phosphorus in phosphate-treated starches. DSC and RVA analyses demonstrated modification-dependent changes in thermal and pasting properties. Overall, the three modification approaches altered starch composition, molecular organization, and functional behaviour without disrupting the fundamental polysaccharide structure. These findings demonstrate the potential of underutilized tropical starches as renewable functional materials and provide a basis for evaluating their corrosion-inhibition performance.

Keywords: Modified starch, Hydroxypropylation, Cross-linking, Dual modification, Tropical tubers

INTRODUCTION

Mild steel corrosion is a major industrial problem in petroleum refining, chemical processing, maritime, pipeline, power plant, and manufacturing industries worldwide. Mild steel is widely used because of its low cost, acceptable mechanical strength, weldability, and ease of manufacture. However, the poor performance in corrosive settings severely limits its long-term industrial applications (Ashmawy and Mostfa, 2021, El-Housseiny et al., 2022). Hydrochloric and sulphuric acid solutions are commonly employed for descaling, pickling, and oil well acidizing. In aggressive acidic environments such as hydrochloric and sulphuric acid solutions, mild steel undergoes accelerated electrochemical degradation, leading to severe material degradation, operational failures, environmental contamination, and increased maintenance costs (Furtado and Nascimento, 2021). As a result, corrosion-related losses have become a major economic and engineering problem worldwide and require attention.

Corrosion inhibitors are among the most practical and cost-effective corrosion-control solutions for protecting metals in aggressive media. The most important inhibitors of corrosion are synthetic organic compounds containing heteroatoms (N, S, O, P) which adsorb on metal surfaces and prevent anodic and cathodic reactions (Ahmed et al., 2024). However, several synthetic inhibitors have been associated with environmental toxicity, low biodegradability, high cost, and ecological persistence, which has led to increasing environmental and regulatory concerns (Verma et al., 2024). Thus, the growing worldwide focus on green chemistry and sustainable industrial practices has increased interest in developing eco-friendly corrosion inhibitors from renewable natural resources.

Natural polymers and biopolymers are being used as alternatives to traditional corrosion inhibitors due to their biodegradability, renewability, low toxicity, availability, and environmentally advantageous properties (Salim et al., 2026). Biopolymers such as starch have received increasing attention because of their abundance, low cost, non-toxicity, and good film-forming properties. Starch, a polysaccharide made up of amylose and amylopectin joined by α-(1→4) and α-(1→6) glycosidic linkages, respectively, has many hydroxyl groups that can adsorb onto metal surfaces (Gamage et al., 2022). Adsorption of starch molecules on mild steel surfaces can form barriers that block charge-transfer reactions and decrease corrosion rates in acid media.

However, direct application of native starches in corrosion inhibition applications is often limited due to their low

mechanical strength, poor thermal stability, high retrogradation tendency; limited solubility control, and poor resistance to harsh acidic environments (Korniy et al., 2023). Under industrial conditions, these restrictions may impair protective performance and decrease adsorption efficacy. To overcome these limitations, researchers have developed several starch-modification methods to improve the physicochemical and functional properties of starches for advanced industrial applications.

Chemical treatment alters starch's molecular structure, enhances stability, improves intermolecular interactions, and increases its adsorption capacity on metallic surfaces. Starch modification methods such as crosslinking and hydroxypropylation have attracted much industrial attention. Crosslinking is the formation of covalent bonds between starch molecules, which confers increased structural strength, decreased solubility, improved acid resistance, and enhanced thermal stability (Awoyale et al., 2026, He et al., 2023). Hydroxypropylation introduces hydroxypropyl groups into the starch structure, thereby strengthening flexibility, hydration properties, swelling behaviour, and adsorption characteristics (Amaraweera et al., 2021). Recently, dual-modification strategies combining two modification processes have attracted interest, offering synergistic improvements in functionality and protective properties beyond those of single modifications. Dual-modified starches can provide better adsorption, film formation, and higher corrosion-inhibition efficiency in severe acidic environments. The starch source, molecular structure, amylose-amylopectin ratio, granule morphology, degree of substitution, and type of modification employed substantially affect the corrosion-inhibiting capabilities of starch-based materials (Wang et al., 2020). Tuber crops are important renewable sources of industrial starches with high starch content and diverse physicochemical properties. However, certain underutilized tuber crops with significant industrial potential have not been sufficiently explored for corrosion inhibition. In particular, water yam (*Dioscorea alata*), trifoliate yam (*Dioscorea dumetorum*), and tigernut (Cyperus esculentus) are potential starch sources with unique compositional and functional properties that could support their use as sustainable corrosion inhibitors (Ogunbiyi et al., 2026). Water yam starch has very high amylose content, good swelling properties, and great film-forming properties, which may enhance adsorption on metal surfaces. Trifoliate yam starch has unique structural features and excellent thermal stability, while tigernut starch has good hydration and functional properties that may promote inhibitor–metal interactions. The different physicochemical properties of these starches help to compare and improve the corrosion inhibition performance after chemical modification (Wu et al., 2024).

Corrosion inhibitors based on modified starches derived from native tuber crops offer significant environmental and economic benefits. Converting renewable agricultural resources into value-added materials for industry aligns with the principles of sustainable development, the circular economy, and green industrial chemistry. Locally grown tuber crops could reduce dependence on imported synthetic corrosion inhibitors and enhance agricultural valorization and industrial sustainability in developing countries (Azima et al., 2020).

Many investigations have been carried out on natural polymers and starch derivatives as green corrosion inhibitors for mild steel in acidic medium (Talha, 2025). However, little or no research has examined the comparative efficacy of corrosion inhibition by modified starches from water yam, trifoliate yam, and tiger nut. The influence of crosslinking, hydroxypropylation, and dual modification on the corrosion-protection properties of these starches remains insufficiently studied. Understanding the relationship between starch modification and corrosion-inhibition efficiency is important for designing efficient bio-based inhibitors for industrial applications.

This work focused on creating and evaluating modified starches from water yam, trifoliate yam, and tigernut as potential sustainable corrosion inhibitors for mild steel. This study investigated the effects of crosslinking, hydroxypropylation, and dual modification on the physicochemical parameters and potential corrosion inhibition efficiency of starches. The results are projected to contribute to the development of environmentally friendly corrosion control systems and extend the industrial applications of underexploited tuber starches.

MATERIALS AND METHODS

Materials

Tiger nut (Cyperus esculentus), trifoliate yam (Dioscorea dumetorum), and water yam (Dioscorea alata) tubers were sourced from farms in Ilara-Mokin (Ondo State), Edo State, and Igbudu Market, Warri (Delta State), respectively, in Nigeria. Figure 1 displays images of the crops grown from tubers. All reagents and chemicals were analytical grade. Sigma-Aldrich (USA) supplied the sodium metabisulfite ($Na_2S_2O_5$), oxalic acid, and ammonium oxalate. Preparation for use included complete washing, rinsing with distilled water, and oven drying of all glassware.

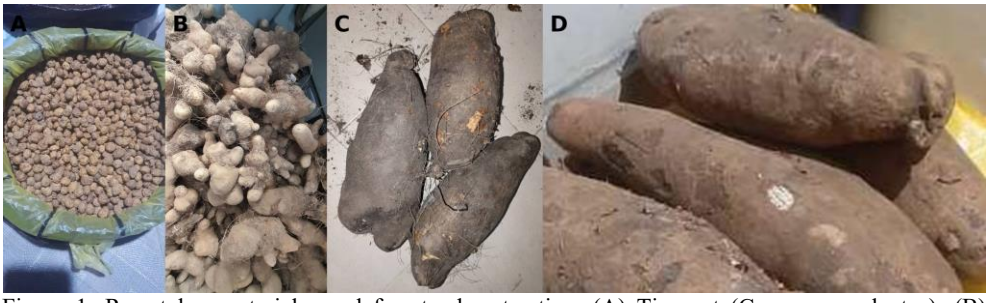


Figure 1: Raw tuber materials used for starch extraction: (A) Tigernut (Cyperus esculentus); (B) Trifoliate yam (Dioscorea dumetorum); (C) Water yam variety 1 (Dioscorea alata); (D) Water yam variety 2 (Dioscorea alata) (Awoyale et al., 2026)

Isolation of Native Starches

The raw materials for starch extraction were fresh tuber crops, with an initial quantity of 12.0 kg of tigernut (Cyperus esculentus), 12.6 kg of water yam (variety 1, Dioscorea alata), 15.5 kg of water yam (variety 2, Dioscorea alata), and 27.0 kg of trifoliate yam (Dioscorea dumetorum) (fresh weight post-peeling). The method of Ishiwu et al. (2017) was used to isolate the starch from the yam tubers, with several modest

modifications. The tubers were rinsed, peeled, and cut into small cubes. They were then soaked in a 0.075% $Na_2S_2O_5$ solution for three hours and subsequently wet-milled using a 10% solution (oxalic acid plus ammonium oxalate) in a 1:1 ratio. After blending, the mélange was suspended in a 10% solution of oxalic acid and ammonium oxalate (1:1) for 12 hours. It was then filtered through muslin cloth. The impure sedimented starch was rinsed repeatedly with distilled water until the pH reached neutral; the supernatant was decanted, and the filtrate was allowed to settle. The starch cake was dried in a dehydrator at 40°C for three days and subsequently preserved in an airtight container for subsequent analyses. The liquid extraction method described by Olatidoye et al. (2019) was used to extract native starch from tigernut tubers (Cyperus esculentus), with minor modifications. The cleansed tubers were soaked in a 0.075% (w/v) $Na_2S_2O_5$ solution at room temperature for 72 hours. During steeping, the soaking solution was replaced every 10 hours. After steeping, the tubers were wet-milled with a 0.075% (w/v) $Na_2S_2O_5$ solution to produce a uniform slurry. The supernatant was decanted after the slurry was filtered through muslin cloth and allowed to settle. A pure, white starch sediment was obtained by subjecting the moist, crude starch cake to multiple washing cycles, which included resuspension in distilled water, filtration, sedimentation, and decantation. Finally, the pure, wet starch cake was dried in a dehydrator at 40°C for 72 hours and then stored in an airtight container for subsequent processing and analysis.

Modification of Starch Samples

To improve the functional properties and broaden the potential applications of the isolated starches, hydroxypropylation, cross-linking, and dual modification (hydroxypropylation followed by cross-linking) were carried out using established procedures with slight modifications. The preparation methods for each modified starch are described below.

Preparation of Hydroxypropylated Starch

The procedure was adapted from the method of Woggum et al. (2015) with slight modifications . Native starch (100 g, dry basis) was suspended in 200 mL of distilled water containing 20 g sodium sulfate (Na_2SO_4) to prepare a uniform slurry. The pH was adjusted to 10.5 using 1 M sodium hydroxide (NaOH), after which propylene oxide (10 %, v/w, based on starch weight) was added. The reaction mixture was incubated in a shaking incubator at 40 °C and 200 rpm for 24 h to facilitate hydroxypropylation. The reaction was terminated by adjusting the pH to 5.0 with 1 M hydrochloric acid (HCl). The modified starch was recovered by centrifugation (10,000 rpm, 15 min), washed repeatedly with distilled water to remove residual reagents, and oven-dried at 40 °C for 48–72 h. The dried starch was milled, passed through a fine mesh sieve, and stored in airtight containers until further analysis.

Preparation of Cross-linked Starch

Cross-linked starch was prepared by the method of Lawal (2004) with slight modification. 100 g (dry basis) of native starch was suspended in 250 mL of distilled water with 10% (w/w) sodium sulphate (Na_2SO_4). Sodium trimetaphosphate (STMP, 2%) and sodium tripolyphosphate (STPP, 5%) were used as cross-linking agents relative to the starch weight. The pH of the slurry was adjusted to 11.0 with 1 M NaOH, and the reaction mixture was incubated at 45 °C for 3 h in a shaking incubator with constant agitation. The process was stopped by changing the pH to 6.5 with 1 M HCl. The modified starch was collected by centrifugation, washed several times with distilled water to remove residual phosphate salts, oven-dried at 40 °C for 24 h, milled, sieved and stored in airtight containers for further analysis.

Preparation of Dual-Modified Starch (Hydroxypropylation–Crosslinking)

Dual-modified starch was prepared by sequential hydroxypropylation followed by cross-linking, as described by Gunaratne and Corke (2007), with slight modifications. Briefly, 100 g (dry basis) of native starch was dispersed in 20% sodium sulfate solution to obtain a 40% (w/v) starch suspension. The slurry pH was adjusted to 10.5 with 5% NaOH before adding propylene oxide at 10% (v/w, based on starch weight). The reaction mixture was stirred for 30 min at room temperature, then incubated at 40 °C with continuous shaking (200 rpm) for 24 h. Following hydroxypropylation, sodium trimetaphosphate (STMP, 2%) and sodium tripolyphosphate (STPP, 5%), based on starch weight, were added to each hydroxypropylated starch slurry. The reaction mixture was stirred for an additional 30 min, after which the pH was adjusted to 5.5 using 10% HCl before incubation at 40 °C and 200 rpm for a further 24 h. The modified starch was recovered by centrifugation (2,500 rpm, 15 min), washed repeatedly with distilled water until free of residual chemicals, and oven-dried at 40 °C for 48–72 h. The dried starch was milled, sieved, and stored in airtight containers until further characterisation.

Functional Properties of the Modified Starches

Bulk Density

The bulk density of the sample was determined using the method described by Chandra et al. (2015). 10 g of the sample was weighed into a 50 ml graduated measuring cylinder. The sample was packed by gently tapping the cylinder on the bench top 10 times from a height of 5 cm. The volume of the sample was recorded. The bulk density was then determined using equation 1.

$$\text{Bulk density (g/ml or g/cm}^3\text{)} = \frac{\text{Weight of sample}}{\text{Volume of sample after tapping}} \quad (1)$$

Swelling Power and Solubility Index

The swelling power and solubility index of the sample were determined using the method described by Xiang et al. (2022). One gram of starch was weighed into a 50 mL centrifuge tube. 50 mL of distilled water was added and mixed gently. The slurry was heated in a water bath at 90 ºC for 50 min. During heating, the slurry was stirred gently to prevent flour clumping. After 15 min, the tube containing the paste was centrifuged at 3,000 rpm for 10 min using an Eppendorf centrifuge (5702R, Germany). The supernatant was decanted immediately after centrifugation. The sediment weight was measured and recorded. The moisture content of the sediment gel was then determined to obtain the gel's dry matter content. Equations 2 and 3 show the solubility index and swelling power, respectively.

$$\text{Solubility index (\%)} = \text{Weight of dry solid after drying} \times 100 \quad (2)$$

$$\text{Swelling power} = \frac{\text{Weight of wet mass of sediment}}{\text{Weight of dry matter in gel}} \quad (3)$$

Water Absorption Capacity

Water absorption capacity of the starch samples was determined using the procedure described by Karmakar et al. (2025) with slight modifications. 1 g of the starch was mixed with 10 ml of water in a centrifuge tube and allowed to stand at room temperature (30 ± 2 ºC) for 1 h. It was then

centrifuged at 2000 rpm for 30 min. The volume of water on the sediment was measured. Water absorption capacities were calculated as the amount of water absorbed per gram of starch, in milliliters.

Oil Absorption Capacity

Oil absorption capacity of the modified starch samples was determined by Okekunle's (2020) method. 1 g of the flour was mixed with 10 mL of oil in a centrifuge tube and allowed to stand at room temperature (30 ± 2 ºC) for 1 h. It was then centrifuged at 2000 rpm for 30 min. The volume of water or oil on the sediment was measured. Oil absorption capacities were calculated as mL of oil absorbed per gram of starch.

Amylose Content

The amylose content of the samples was determined based on the iodine colourimetric method as described by Amoo et al. (2014). Approximately 0.1 g of the starch sample was solubilized in 1 mL of 95% ethanol and 9 mL of 1 N NaOH, and then heated in a boiling water bath for 10 min. Subsequently, 1 mL of the extract was diluted to 10 mL with distilled water. To 0.5 mL of the diluted extract, 0.1 mL of 1 N acetic acid and 2 mL iodine solution (0.2 g I_2 + 2.0 g KI in 100 mL of distilled water) were added to develop a dark blue colour. The coloured solution was made up to 10 mL with distilled water and allowed to stand for 20 min for complete colour development. The solution was vortexed, and its absorbance was read on a spectrophotometer at 620 nm. The absorbance of a standard amylose solution with a known amylose concentration was used to estimate amylose content, expressed as % (dry basis) as shown in equation 4.

$$\% \text{ Amylose} = \frac{\% \text{ amylose of standard x Absorbance of sample}}{\text{Absorbance of standard}} \quad (4)$$

Pasting Properties of Starch Samples

Pasting characteristics were determined with a Rapid Visco Analyzer (RVA TECMASTER, perten instrument). Parameters estimated were peak viscosity, trough viscosity, breakdown viscosity, final viscosity, setback, pasting temperature, and time to reach peak viscosity. Of the sample, 3.50 g was weighed to the nearest 0.01 g into a vessel before being transferred into the test canister, and 25 mL of distilled water was dispensed into the canister. The sample was mixed thoroughly so that no lumps formed. A paddle was then placed into the canister, and the test proceeded immediately, automatically plotting the characteristic curve.

Fourier Transform Infrared (FT- IR) spectroscopy

Fourier Transform Infrared (FTIR) spectroscopy was employed to characterize the chemical structure, identify the functional groups, and evaluate the structural integrity of the native starch samples. Spectral analysis was performed using a Nicolet iS20 FTIR spectrometer (2024 model, Thermo Fisher Scientific, USA). Before analysis, the instrument was calibrated according to the manufacturer's specifications, and spectra were acquired over the appropriate mid-infrared region. The obtained spectra were processed and analyzed using OMNIC™ software (Thermo Fisher Scientific, USA). Characteristic absorption bands corresponding to hydroxyl, C–H, O–H bending, and glycosidic C–O–C stretching vibrations were identified and compared to assess the molecular structure and detect any structural variations among the starch samples.

X-ray Diffraction Pattern (XRD) and Relative Crystallinity (Crl %)

The X-ray diffraction patterns of the starch samples were obtained utilizing an X-ray diffractometer (D8 Advance Eco, Bruker) in accordance with a previously established method (Yadav et al. 2024). The instrument was utilized at 40 kV and 40 mA, employing Cu-Kα radiation (λ = 0.15406 nm) across a scanning angle range of 3-30° (2θ). The relative crystallinity (Crl) was calculated using the following formula.

$$\text{Crl (\%)} = \text{Relative crystallinity (\%)} = \frac{Ac}{Ac+Aa} \text{ x } 100 \quad (5)$$

Ac and Aa represent the area of the crystalline portion, while Aa represents the area of the amorphous zone. The Crl values were computed using Origin2025b SR1 software (Built 10.25.234 OriginLab Corporation)

Scanning Electron Microscopy (SEM) Analysis of Modified Starch Granules

Morphological properties of starch granules were observed by scanning electron microscopy (Axia ChemiSEM 2023 model, Thermo Fisher Scientific, USA). The starch powders were attached to aluminium stubs with double-sided conductive carbon adhesive tape and coated with a tiny layer of platinum to improve the electrical conductivity and reduce charging during imaging. The samples were investigated in a high-vacuum system at an accelerating voltage of 3.0 kV, and micrographs were recorded at magnifications of ×100, ×500, and ×1000 to enable detailed observation of granule microstructure and surface morphology. Qualitative assessment of representative micrographs was conducted to evaluate granule form, size distribution, surface properties, structural integrity, and degree of granule aggregation after the various starch modification treatments.

Differential Scanning Calorimetry (DSC)

The thermal (gelatinization) properties of the native and modified starch samples were determined using a METTLER TOLEDO DSC 1 differential scanning calorimeter (METTLER TOLEDO, Switzerland), operated using STARe software version 13.00, following the method described by Olayinka et al. 2015 with modifications. Approximately 2.0 mg of starch sample (dry-weight basis) was accurately weighed into an aluminum DSC pan, and 6.0 µL of distilled water was added using a micro syringe. The pan was hermetically sealed and equilibrated at 30 ± 2 °C for 24 h to ensure adequate hydration and uniform water distribution within the starch sample. The equilibrated samples were heated from 30 to 140 °C at a heating rate of 10 °C min^{-1}, using an empty sealed aluminum pan as the reference. The resulting thermograms were analyzed using the STARe software to determine the onset gelatinization temperature (T_o), peak gelatinization temperature (T_p), conclusion gelatinization temperature (T_c), and gelatinization enthalpy (ΔH). The gelatinization enthalpy was determined from the integrated area under the endothermic peak and expressed as J g^{-1} of dry starch.

Statistical Analysis of Results

Statistical analyses were performed in Python using SciPy 1.14.1 and statsmodels 0.14.4.

RESULTS AND DISCUSSION

Proximate Composition of the Modified Starches

Table 1 shows the proximate compositions, pH, and apparent amylose contents of the modified starches. Chemical treatment dramatically altered moisture, ash, pH, and

apparent amylose content. Fat and protein levels were often not affected, whereas crude fibre was not detected in any of the samples. The low levels of non-starch components across the samples indicate that hydroxypropylation, cross-linking, and dual modification preserved starch as the major component, retaining abundant hydroxyl-rich polysaccharide chains essential for adsorption on metal surfaces. Cross-linked starches always showed the lowest moisture contents. Thus, water accessibility was limited as intermolecular cross-links were formed, restricting chain mobility and hydration. In contrast, hydroxypropylated starches showed significantly higher moisture levels, reflecting the increased hydrophilicity conferred by hydroxypropyl groups. Similar behaviours have been observed with chemically treated starches, where cross-linking improves structural stiffness, and hydroxypropylation increases water affinity (Punia Bangar et al., 2024). Cross-linked and dual-modified starches, in general, have greater ash content, perhaps due to residual mineral species involved with the modification process. The comparatively low ash concentrations observed indicate that the starch matrix remained largely intact and suitable for adsorption-based corrosion prevention, while excessive inorganic residues can affect electrolyte conductivity.

The greatest modifying effect was observed in perceived amylose content. Crosslinked starches consistently showed the highest apparent amylose levels, hydroxypropylated starches the lowest, and dual-modified starches intermediate. This trend reflects changes in starch molecular organization and iodine-binding properties induced by modification, not the production of additional amylose molecules (Kibar et al., 2024). Significant differences were also detected among modification treatments in pH values. Hydroxypropylated starches were mostly near neutral, but cross-linked starches were somewhat acidic, indicating the chemistry of the modification process. Powder pH alone does not determine corrosion inhibition, although it may affect starch stability and adsorption behaviour under the acidic conditions typically encountered in corrosion tests.

The compositional changes confirmed that chemical modification improved the starches' physicochemical properties without compromising their high carbohydrate purity. Cross-linking gave the most advantageous combination of low moisture and high apparent amylose among the treatments, suggesting potential for more stable adsorption-film development. Dual modification may provide a compromise between water dispersibility and structural stability. These features suggest the modified starches may be applicable as durable polymeric corrosion inhibitors, but electrochemical experiments are needed to establish their inhibition efficiency.

Table 1: Proximate Composition, pH, and Apparent Amylose Content of Modified Starches

Source	Sample	Moisture (%)	Ash (%)	Fat (%)	Protein (%)	Crude fibre	Carbohydrate (%)	pH	Amylose (%)
Water yam 1	SMH	12.31 ± 0.02^{a}	0.20 ± 0.02^{a}	0.09 ± 0.02^{a}	0.10 ± 0.02^{a}	ND	87.30 ± 0.04^{b}	6.90 ± 0.03^{a}	25.40 ± 0.02^{c}
	SMC	12.12 ± 0.02^{b}	0.23 ± 0.03^{a}	0.10 ± 0.02^{a}	0.10 ± 0.00^{a}	ND	87.45 ± 0.03^{a}	6.00 ± 0.02^{c}	27.80 ± 0.02^{a}
	SMD	12.33 ± 0.02^{a}	0.25 ± 0.02^{a}	0.09 ± 0.03^{a}	0.10 ± 0.00^{a}	ND	87.23 ± 0.03^{b}	6.20 ± 0.02^{b}	27.30 ± 0.02^{b}
Water yam 2	SRH	12.35 ± 0.02^{a}	0.20 ± 0.02^{b}	0.09 ± 0.03^{a}	0.10 ± 0.02^{a}	ND	87.26 ± 0.05^{a}	6.90 ± 0.03^{a}	24.00 ± 0.03^{c}
	SRC	12.24 ± 0.02^{b}	0.25 ± 0.02^{a}	0.10 ± 0.02^{a}	0.10 ± 0.03^{a}	ND	87.31 ± 0.09^{a}	6.00 ± 0.02^{c}	26.50 ± 0.03^{a}
	SRD	12.37 ± 0.03^{a}	0.28 ± 0.02^{a}	0.09 ± 0.02^{a}	0.09 ± 0.03^{a}	ND	87.17 ± 0.00^{a}	6.10 ± 0.02^{b}	26.10 ± 0.02^{b}
Trifoliate yam	SUH	12.65 ± 0.02^{a}	0.19 ± 0.03^{b}	0.09 ± 0.02^{a}	0.08 ± 0.03^{a}	ND	86.99 ± 0.06^{a}	7.05 ± 0.03^{a}	25.20 ± 0.03^{c}
	SUC	12.43 ± 0.03^{c}	0.28 ± 0.02^{a}	0.10 ± 0.03^{a}	0.10 ± 0.02^{a}	ND	87.09 ± 0.10^{a}	6.00 ± 0.03^{c}	29.45 ± 0.03^{a}
	SUD	12.55 ± 0.03^{b}	0.30 ± 0.02^{a}	0.05 ± 0.03^{a}	0.08 ± 0.02^{a}	ND	87.02 ± 0.00^{a}	6.90 ± 0.02^{b}	28.50 ± 0.03^{b}
Tigernut	SNH	12.80 ± 0.02^{a}	0.20 ± 0.02^{b}	0.10 ± 0.02^{a}	0.10 ± 0.03^{a}	ND	86.80 ± 0.05^{b}	7.30 ± 0.03^{a}	22.94 ± 0.02^{c}
	SNC	12.41 ± 0.03^{c}	0.38 ± 0.03^{a}	0.10 ± 0.00^{a}	0.10 ± 0.02^{a}	ND	87.01 ± 0.08^{a}	5.80 ± 0.03^{c}	24.70 ± 0.02^{a}
	SND	12.70 ± 0.02^{b}	0.42 ± 0.02^{a}	0.07 ± 0.02^{a}	0.05 ± 0.02^{a}	ND	86.76 ± 0.03^{b}	6.80 ± 0.02^{b}	24.40 ± 0.03^{b}

Values are expressed as mean ± standard deviation (n = 3). Within each botanical source and parameter, means bearing different superscript letters differ significantly (one-way ANOVA followed by Tukey's HSD test, $p < 0.05$). Superscripts are not intended for comparison among different botanical sources. ND = not detected. Hydroxypropylated: SMH, SRH, SUH and SNH; cross-linked: SMC, SRC, SUC and SNC; dual-modified: SMD, SRD, SUD and SND.

Functional Properties of Modified Starches

The usefulness of starch for industrial applications is determined by its functional qualities, which are related to its hydration behaviour, adsorption characteristics, dispersion stability and interaction with surrounding fluids. The chemical modification significantly ($p < 0.05$) influenced the water absorption capacity (WAC), oil absorption capacity (OAC) and water binding capacity (WBC) of the starches, as shown in Table 2, while loose and tapped bulk densities were not statistically altered ($p > 0.05$), suggesting that the modification mainly affected the molecular structure and not the particle packing properties. Hydroxypropylation produced the highest WAC regardless of botanical origin, whereas cross-linked starches showed the lowest values. Hydroxypropylated water yam 1 had the highest WAC (2.99 ± 0.03 g g-1) among the modified starches, followed by hydroxypropylated water yam 2 (2.80 ± 0.02 g g-1), whereas cross-linked trifoliate yam starch had the lowest WAC (1.75

± 0.03 g g-1). Intermediate values of 2.10 to 2.83 g g-1 were always obtained for dual-modified starches. The rise in WAC after hydroxypropylation is due to the introduction of hydrophilic hydroxypropyl groups, which weaken the native intermolecular hydrogen-bonding network, increase the free volume in starch granules, and allow easier water penetration. In contrast, the phosphate cross-links produced by STMP/STPP treatment strengthen the molecular network, prevent chain mobility, and diminish granule swelling, thereby reducing water uptake. Similar findings were found for hydroxypropylated and dual-modified cereal and tuber starches, where hydroxypropyl substitution increased hydration, and cross-linking increased structural rigidity (Kibar et al., 2024, Lagunes-Delgado et al., 2024). Oil absorption capacity showed a similar, albeit less pronounced, trend. Typical OAC values for hydroxypropylated and dual-modified starches were substantially greater than those for their cross-linked counterparts. Water yam 1 and trifoliate yam dual-modified starches showed the highest OAC (1.30 ± 0.03 g g-1), while cross-linked tigernut starch had the lowest (0.80 ± 0.03 g g-1). The rise in OAC indicates that chemical alteration affected the spatial structure of amylose and amylopectin chains, hence exposing more non-polar zones that might interact with hydrophobic substances. Previously, hydroxypropyl substitution was shown to increase molecular flexibility and improve access to internal binding sites, thereby improving oil retention (Punia Bangar et al., 2024). Similarly, dual modification appears to combine the advantageous effects of hydroxypropylation with the structural enhancement provided by phosphate cross-linking. Significant variations in WBC in modified starches were also noted. Hydroxypropylated tigernut starch exhibited the highest WBC (1.48 ± 0.03 g g^{-1}), followed by hydroxypropylated trifoliate yam (1.29 ± 0.02 g g^{-1}), but cross-linked water yam 2 exhibited the lowest value (1.00 ± 0.03 g g^{-1}). The consistently higher WBC of hydroxypropylated starches implies that hydroxypropyl substitution increased starch molecules' ability to retain water within the polymer network by increasing the availability of hydroxyl groups. Conversely, cross-linking reduced molecular flexibility and hindered water immobilization by constraining starch-matrix expansion. These findings agree with previous reports showing that hydroxypropylation increases hydration capacity, while phosphate cross-linking suppresses excessive water retention by reinforcing intermolecular associations (Kibar et al., 2024). In corrosion inhibition, a high WBC is favorable because bound water helps build stable hydrated polymer coatings on metallic surfaces. Such hydrated coatings can serve as diffusion barriers that minimize electrolyte penetration and minimize the transit of corrosive ions to the metal contact. However, an overly moist network can slowly lose its mechanical integrity when exposed for a long time. Thus, the intermediate WBC values observed for the dual-modified starches may represent an ideal compromise between sufficient hydration to adsorb and sufficient structural stability to form a persistent protective coating. Unlike the hydration-related features, the chemical change did not appreciably affect the loose and tapped bulk densities. The loose bulk density ranged from 0.58-0.68 g mL-1, whereas the tapped bulk density ranged from 0.69-0.79 g mL-1 for all modified starches. No significant alterations were found, indicating that hydroxypropylation and cross-linking mostly affected the internal molecular organization rather than the outward shape or packing behaviour of the starch granules. This insight is useful for industrial applications because starch powders with identical bulk densities can be processed, transported, and formed under similar production conditions without major changes to equipment or processing parameters. In corrosion inhibitor formulations, constant bulk density also gives predictable dispersion characteristics and homogeneous dosing during industrial application. The results demonstrate that hydroxypropylation was the most effective modification for improving hydration-related functional properties, whereas cross-linking produced structurally more rigid starches with lower water uptake. Dual modification successfully integrated the desirable characteristics of both treatments by maintaining relatively high WAC, OAC, and WBC while preserving structural stability. This combination is particularly attractive for developing environmentally benign corrosion inhibitors because effective polysaccharide-based inhibitors require rapid hydration, efficient adsorption, and formation of mechanically stable protective films on metallic surfaces. The present findings therefore indicate that the dual-modified starches, particularly those derived from water yam 1 and trifoliate yam, constitute promising candidates for further electrochemical evaluation as sustainable corrosion inhibitors for metallic systems.

Table 2: Functional Properties of Modified Starches

Starch Source	Sample	WAC (g/g)	OAC (g/g)	WBC (g/g)	Loose bulk density (g/mL)	Tapped bulk density (g/mL)
Tigernut	Hydroxypropylated	2.25 ± 0.03^{a}	1.20 ± 0.03^{a}	1.48 ± 0.03^{a}	0.63 ± 0.03^{a}	0.72 ± 0.03^{a}
	Cross-linked	1.80 ± 0.02^{c}	0.80 ± 0.03^{b}	1.26 ± 0.02^{b}	0.61 ± 0.03^{a}	0.70 ± 0.02^{a}
	Dual-modified	2.10 ± 0.02^{b}	1.20 ± 0.02^{a}	1.29 ± 0.02^{b}	0.64 ± 0.02^{a}	0.74 ± 0.03^{a}
Water yam 1	Hydroxypropylated	2.99 ± 0.03^{a}	1.30 ± 0.03^{a}	2.15 ± 0.03^{a}	0.67 ± 0.02^{a}	0.77 ± 0.02^{a}
	Cross-linked	2.30 ± 0.02^{c}	1.21 ± 0.03^{b}	1.70 ± 0.03^{c}	0.66 ± 0.03^{a}	0.75 ± 0.02^{a}
	Dual-modified	2.83 ± 0.02^{b}	1.30 ± 0.03^{a}	1.86 ± 0.02^{b}	0.68 ± 0.03^{a}	0.79 ± 0.02^{a}
Water yam 2	Hydroxypropylated	2.80 ± 0.02^{a}	1.00 ± 0.03^{b}	1.16 ± 0.02^{a}	0.65 ± 0.02^{a}	0.76 ± 0.03^{a}
	Cross-linked	2.10 ± 0.03^{c}	0.90 ± 0.02^{c}	1.00 ± 0.03^{b}	0.64 ± 0.02^{a}	0.75 ± 0.03^{a}
	Dual-modified	2.70 ± 0.03^{b}	1.10 ± 0.03^{a}	1.03 ± 0.03^{b}	0.67 ± 0.03^{a}	0.78 ± 0.02^{a}
Trifoliate yam	Hydroxypropylated	2.30 ± 0.02^{a}	1.00 ± 0.02^{b}	1.29 ± 0.02^{a}	0.59 ± 0.03^{a}	0.70 ± 0.04^{a}
	Cross-linked	1.75 ± 0.03^{c}	1.00 ± 0.03^{b}	1.08 ± 0.03^{b}	0.58 ± 0.02^{a}	0.69 ± 0.03^{a}
	Dual-modified	2.10 ± 0.03^{b}	1.30 ± 0.03^{a}	1.10 ± 0.02^{b}	0.61 ± 0.02^{a}	0.73 ± 0.03^{a}

Values are mean ± standard deviation of triplicate determinations (n = 3). Within each starch source and property column, means carrying different superscript letters differ significantly according to Tukey's HSD test (α = 0.05). The highest mean is assigned superscript a.

Solubility of Modified Starches

Table 3 displays the effect of hydroxypropylation, cross-linking, and dual modification on the solubility (%) of starches from tigernut, water yam 1 and 2, and trifoliate yam, while Table 4 shows the statistical (ANOVA) analysis results. The solubility of all modified starches rose considerably with temperature (55-85 °C). This indicates gradual breaking of hydrogen bonding in starch granules and higher molecular mobility during heating. Such temperature-dependent increases are commonly observed in chemically modified starches, as thermal energy promotes granule expansion, amylopectin relaxation, and leaching of amylose into the surrounding medium (Mehfooz et al., 2020). Hydroxypropylated starches showed the highest solubility, regardless of botanical source. The greatest value (8.62%) was observed in Trifoliate yam (SUH) at 85 °C. The hydroxypropyl groups provide bulky hydrophilic substituents that reduce intermolecular hydrogen bonding, lower crystallinity, and allow more water to penetrate the starch granules. This behaviour is in agreement with studies published for hydroxypropylated yam, cassava and potato starches where hydroxypropylation greatly enhanced water solubility by increasing the amorphous regions within the starch matrix (Chen et al., 2021). In general, the modified samples were less soluble than native starches, and cross-linked starches were the least soluble. Cross-linking forms covalent bonds between neighbouring starch molecules, strengthening the granule structure and reducing polymer escape when heated. Thus, even at higher temperatures, water penetration is limited. Therefore, these results align with many reports showing that phosphate cross-linking enhances structural stiffness and reduces starch dissolution (Chandak et al., 2022). The dual-modified starches presented behaviour between the hydroxypropylated and cross-linked starches. The hydroxypropyl substituents and the phosphate cross-links appear to balance increased hydration with enhanced structural stability, giving a modest but controlled solubility. This behaviour has been described for dual-modified cereal and tuber starches where hydroxypropylation counteracts the rigidity conferred by cross-linking, resulting in starches with improved processing stability (Mehfooz et al., 2021). However, no significant changes ($p > 0.05$) were seen among the Water yam 2 starches at 55 °C, showing that chemical alteration had little effect before considerable granule swelling began. However, at higher temperatures, considerable variation was observed, reflecting the increasing expression of structural changes once gelatinization began. The observed solubility behaviour is of special interest from the point of view of green corrosion inhibition. Highly soluble hydroxypropylated starches are expected to dissolve rapidly under acidic conditions, helping transport and adsorb hydroxyl-rich polymer chains on metal surfaces, where they can form protective adsorption coatings (Deng et al., 2021, Chen et al., 2024). On the other hand, the relatively low solubility of cross-linked starches indicates a slower dissolution but a possibly better persistence of the adsorbed protective coating due to their higher structural integrity. Therefore, dual-modified starches could be the most attractive compromise, showing satisfactory aqueous dispersibility together with better film stability, properties particularly wanted for eco-friendly corrosion inhibitors in long-term exposures. The results demonstrate that hydroxypropylation enhances starch-water interactions, whereas cross-linking restricts polymer dissolution. The complementary effects achieved through dual modification suggest considerable potential to tailor starch performance to the requirements of sustainable corrosion inhibitor formulations.

Table 3: Solubility (%) of Hydroxypropylated, Cross-Linked, and Dual-Modified Starches

Starch source	Sample	Solubility (%)			
		55 °C	65 °C	75 °C	85 °C
Tigernut	SNH	3.90 ± 0.03^{a}	4.35 ± 0.03^{a}	6.17 ± 0.02^{a}	7.20 ± 0.03^{a}
	SNC	3.00 ± 0.02^{b}	4.03 ± 0.02^{b}	5.03 ± 0.03^{b}	6.19 ± 0.02^{b}
	SND	2.99 ± 0.02^{b}	3.43 ± 0.02^{c}	4.51 ± 0.04^{c}	5.96 ± 0.05^{c}
Trifoliate yam	SUH	4.42 ± 0.02^{a}	5.10 ± 0.03^{a}	6.52 ± 0.03^{a}	8.62 ± 0.03^{a}
	SUC	3.10 ± 0.03^{c}	4.20 ± 0.02^{c}	6.10 ± 0.02^{c}	6.76 ± 0.02^{c}
	SUD	3.30 ± 0.03^{b}	4.51 ± 0.02^{b}	6.30 ± 0.02^{b}	7.00 ± 0.03^{b}
Water yam 1	SMH	3.20 ± 0.03^{a}	5.10 ± 0.02^{a}	6.20 ± 0.03^{a}	7.00 ± 0.03^{a}
	SMC	3.10 ± 0.03^{b}	4.10 ± 0.02^{b}	5.70 ± 0.03^{c}	6.80 ± 0.02^{b}
	SMD	3.00 ± 0.02^{c}	4.00 ± 0.03^{c}	5.93 ± 0.03^{b}	6.98 ± 0.03^{a}
Water yam 2	SRH	3.00 ± 0.03^{a}	4.98 ± 0.03^{a}	5.94 ± 0.02^{a}	7.10 ± 0.02^{a}
	SRC	2.99 ± 0.03^{a}	4.00 ± 0.03^{c}	5.08 ± 0.03^{b}	7.00 ± 0.03^{b}
	SRD	3.00 ± 0.02^{a}	4.10 ± 0.02^{b}	5.94 ± 0.03^{a}	7.10 ± 0.03^{a}

Values are mean ± standard deviation of triplicate determinations (n = 3). Within each starch source and temperature column, means bearing different superscript letters differ significantly according to Tukey's HSD test ($\alpha = 0.05$); means sharing at least one letter are not significantly different. Sample codes: SNH, SNC and SND = hydroxypropylated, cross-linked and dual-modified tigernut starch; SUH, SUC and SUD = corresponding trifoliate yam starches; SMH, SMC and SMD = corresponding water yam 1 starches; SRH, SRC and SRD = corresponding water yam 2 starches

Table 4: One-way ANOVA Summary for Solubility of Modified Starches

Starch source	Temperature	df between	df within	F-value	p-value	Decision
Tigernut	55 °C	2	6	1445.47	<0.0001	Significant
Tigernut	65 °C	2	6	1154.82	<0.0001	Significant
Tigernut	75 °C	2	6	2237.38	<0.0001	Significant
Tigernut	85 °C	2	6	1030.50	<0.0001	Significant
Trifoliate yam	55 °C	2	6	2070.55	<0.0001	Significant

Starch source	Temperature	df between	df within	F-value	p-value	Decision
Trifoliate yam	65 °C	2	6	1106.65	<0.0001	Significant
Trifoliate yam	75 °C	2	6	233.65	<0.0001	Significant
Trifoliate yam	85 °C	2	6	4187.45	<0.0001	Significant
Water yam 1	55 °C	2	6	40.91	0.0003	Significant
Water yam 1	65 °C	2	6	1958.82	<0.0001	Significant
Water yam 1	75 °C	2	6	208.78	<0.0001	Significant
Water yam 1	85 °C	2	6	49.64	0.0002	Significant
Water yam 2	55 °C	2	6	0.14	0.8752	Not significant
Water yam 2	65 °C	2	6	1189.64	<0.0001	Significant
Water yam 2	75 °C	2	6	1008.55	<0.0001	Significant
Water yam 2	85 °C	2	6	13.64	0.0059	Significant

Statistical Analysis

One-way analysis of variance was performed separately for each starch source at each temperature, with modification type as the factor. Tukey's Honestly Significant Difference test was used to separate treatment means at $\alpha = 0.05$. Tukey superscripts were generated from the pairwise significance matrix and verified against all comparisons.

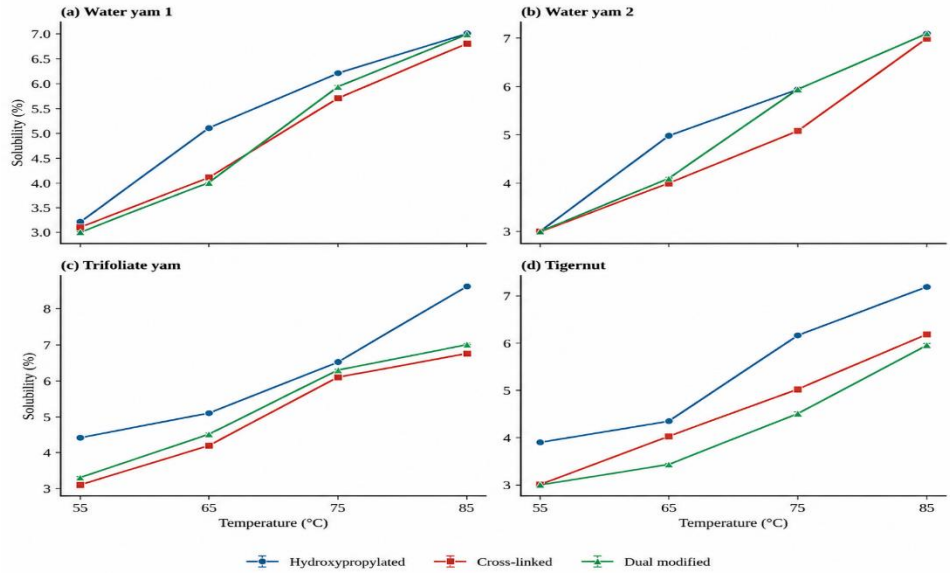


Figure 2: Solubility (%, mean ± SD, n = 3) of hydroxypropylated, cross-linked, and dual-modified starches from (a) water yam cultivar 1, (b) water yam cultivar 2, (c) trifoliate yam, and (d) tigernut as a function of temperature (55–85 °C)

Swelling Power of the Modified Starches

Swelling power increased significantly ($p < 0.05$) with increasing temperature (55–85 °C) in all modified starches, confirming that thermal energy progressively weakened intermolecular hydrogen bonds and promoted water penetration into the starch granules (Tables 5 & 6 and Figure 3). Swelling capabilities of hydroxypropylated (H) and dual-modified (D) starches were significantly higher than those of cross-linked (C) starches, regardless of botanical source. At 85 °C, swelling power ranged from 10.00 to 12.70 g g^{-1}, with the highest values recorded for dual-modified tigernut starch (12.70 g g^{-1}) and hydroxypropylated water yam 1 (12.50 g g^{-1}), whereas cross-linked water yam 1 exhibited the lowest swelling (10.00 g g^{-1}). The data shown here indicate that the hydration behaviour of starches is strongly impacted by the type of chemical modification and the botanical origin. The increased swelling after hydroxypropylation results from inserting hydroxypropyl groups into starch molecules, which disrupt intermolecular hydrogen bonding, reduce crystalline order, and increase the accessibility of hydroxyl groups to water molecules. Consequently, the modified granules hydrate more readily and show greater volumetric expansion after heating. Similar increases in swelling capacity following hydroxypropylation have been reported for sweet potato, apios, and cereal starches, where the improved hydration was associated with increased molecular flexibility and reduced crystallinity (Fu et al., 2019, Parl and Kim, 2020). In contrast, for all starch sources, cross-linking strongly controlled swelling. This behaviour is expected because phosphate bridges formed by STMP/STPP reinforce intermolecular associations between amylose and amylopectin chains, thereby limiting granule expansion and reducing water diffusion into the starch matrix. Phosphate cross-linked starches have also been observed to consistently reduce swelling to a similar extent and, in general, confer greater structural rigidity and thermal stability (Punia Bangar et al., 2024, Kumar et al., 2025). Dual modification resulted in similar or higher swelling capabilities than hydroxypropylation alone, especially in tigernut and water yam 2 starches. This implies that the combined effect of hydroxypropyl substitution and controlled cross-linking created a balanced molecular architecture that retained sufficient hydrophilic sites for water uptake, while the moderately cross-linked network-maintained granule

integrity during heating. Similar synergistic behaviour was also seen in other dual-modified starch systems where regulated cross-link density increased functional performance without overly constraining hydration (Kumar et al., 2025). Differences among the four starch sources also indicated that intrinsic properties of each botanical origin, including amylose content, granule morphology, and crystalline organization, influenced the response to chemical treatment. However, the continuous increase in swelling with temperature for all samples indicates that the modification treatments did not affect the underlying thermal hydration behaviour of the starches, but rather they affected the extent of water uptake. Swelling power is a key functional attribute of corrosion inhibition because appropriate hydration enables polymer chain mobility, adsorption, and the formation of a continuous protective coating on metallic surfaces. Starches with increased swelling capacity are expected to distribute more easily in aqueous media and provide better surface coverage, leading to a superior barrier to corrosive ions. But over-hydration can cause excessive edema and film instability. In this context, dual-modified starches seem particularly desirable, as they offer significant swelling capacity alongside the structural strengthening provided by cross-linking. This balance is predicted to promote the formation of compact, sticky, and mechanically stable protective layers, making these starches promising, ecologically benign corrosion inhibitors.

Table 5: Swelling Power (g/g) of Modified Starches at Different Temperatures

Starch source	Sample	55 °C	65 °C	75 °C	85 °C
Tigernut	SNH	4.20 ± 0.03^{b}	6.80 ± 0.02^{a}	10.50 ± 0.02^{a}	12.40 ± 0.02^{b}
	SNC	3.40 ± 0.02^{c}	5.10 ± 0.02^{c}	8.20 ± 0.02^{c}	10.70 ± 0.02^{c}
	SND	4.60 ± 0.03^{a}	6.70 ± 0.03^{b}	10.30 ± 0.03^{b}	12.70 ± 0.02^{a}
Trifoliate yam	SUH	4.20 ± 0.03^{a}	6.30 ± 0.03^{a}	9.30 ± 0.02^{a}	11.70 ± 0.02^{a}
	SUC	3.60 ± 0.02^{c}	5.30 ± 0.03^{c}	8.50 ± 0.02^{c}	10.30 ± 0.03^{c}
	SUD	3.90 ± 0.03^{b}	5.40 ± 0.02^{b}	8.70 ± 0.02^{b}	10.80 ± 0.02^{b}
Water yam 1	SMH	4.50 ± 0.02^{a}	6.50 ± 0.03^{a}	9.80 ± 0.03^{a}	12.50 ± 0.02^{a}
	SMC	3.20 ± 0.02^{c}	4.50 ± 0.03^{c}	8.10 ± 0.02^{c}	10.00 ± 0.03^{c}
	SMD	4.00 ± 0.02^{b}	6.10 ± 0.03^{b}	9.20 ± 0.02^{b}	11.60 ± 0.02^{b}
Water yam 2	SRH	4.60 ± 0.03^{a}	6.60 ± 0.02^{a}	10.10 ± 0.02^{a}	12.00 ± 0.02^{b}
	SRC	3.70 ± 0.02^{c}	5.80 ± 0.02^{c}	8.60 ± 0.02^{c}	10.80 ± 0.03^{c}
	SRD	4.20 ± 0.02^{b}	6.40 ± 0.03^{b}	9.70 ± 0.02^{b}	12.20 ± 0.02^{a}

Values are mean ± standard deviation of triplicate determinations (n = 3). Within each starch source and temperature column, means followed by different superscript letters are significantly different according to Tukey's HSD test ($\alpha = 0.05$). The highest mean is assigned superscript a. Sample codes: H = hydroxypropylated; C = cross-linked; D = dual modified. SN = tigernut; SU = trifoliate yam; SM = water yam 1; SR = water yam 2

Table 6: One-way ANOVA Summary for Swelling Power

Starch source	Temperature	df_1	df_2	F-value	p-value	Decision
Tigernut	55 °C	2	6	1527.27	7.53e-09	Significant
	65 °C	2	6	4817.65	2.41e-10	Significant
	75 °C	2	6	8594.12	4.25e-11	Significant
	85 °C	2	6	8725.00	4.06e-11	Significant
Trifoliate yam	55 °C	2	6	368.18	5.28e-07	Significant
	65 °C	2	6	1240.91	1.40e-08	Significant
	75 °C	2	6	1300.00	1.22e-08	Significant
	85 °C	2	6	2664.71	1.42e-09	Significant
Water yam 1	55 °C	2	6	3225.00	8.03e-10	Significant
	65 °C	2	6	4157.27	3.75e-10	Significant
	75 °C	2	6	3935.29	4.42e-10	Significant
	85 °C	2	6	8488.24	4.41e-11	Significant
Water yam 2	55 °C	2	6	1076.47	2.15e-08	Significant
	65 °C	2	6	917.65	3.46e-08	Significant
	75 °C	2	6	4525.00	2.91e-10	Significant
	85 °C	2	6	3035.29	9.63e-10	Significant

df_1 = between-group degrees of freedom; df_2 = within-group degrees of freedom. All tests were significant at $p < 0.05$.

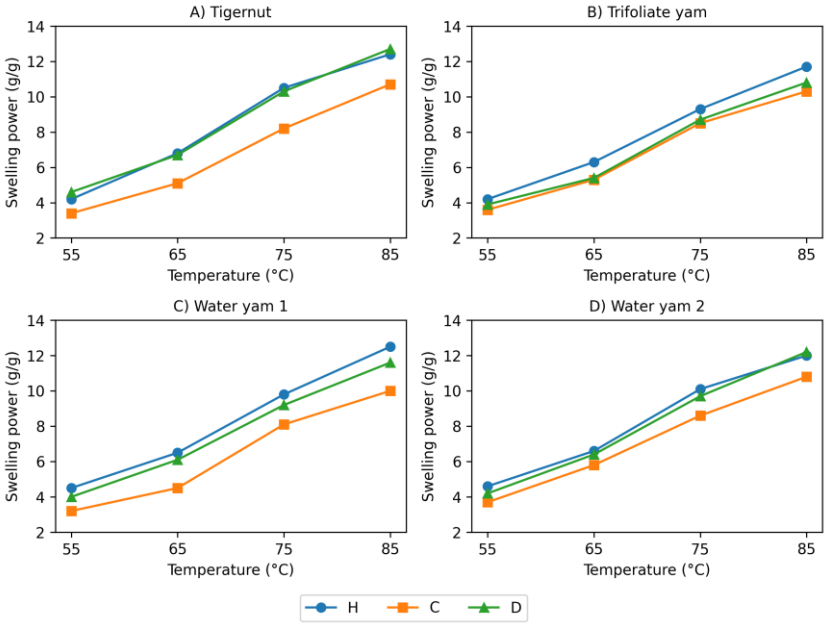


Figure 3: Swelling Power of Modified Starches

Scanning Electron Microscopy (SEM) of Modified Starches

Scanning electron microscopy was used to examine the surface appearance of starch granules from tigernut, water yam, and trifoliate yam, and the effects of hydroxypropylation, cross-linking, and dual modification on their granules. The micrographs (Figure 4) showed that the modified starches exhibited significant morphological changes, suggesting that the chemical treatments affected granule structure in distinct ways. Hydroxypropylated tigernut starch (SUH) granules exhibited aggregation and had coarse, thick surfaces. At higher magnification, granules showed cohesive topologies and reduced interparticle separation. Hydroxypropylation attaches bulky hydroxypropyl groups to the amorphous regions of starch granules, thereby increasing intermolecular spacing and disrupting hydrogen bonds. Similar morphological changes have been reported in hydroxypropylated maize, cassava, and potato starches, where chemical modification resulted in increased surface roughness and granule aggregation due to partial disruption of the native starch structure (Zhang et al., 2024)

Cross-linked tigernut starch (SUC) was denser and more compact than hydroxypropylated starch. The granules were more tightly packed, with fewer visible cracks and fractures, indicating increased structural integrity due to the formation of phosphate bridges. Cross-linking adjacent starch chains with sodium trimetaphosphate (STMP) and sodium tripolyphosphate (STPP) yields covalent linkages between chains and improves granule strength and swelling resistance. Comparable results were also found for the cross-linked potato and rice starches, with phosphate cross-linking producing more compact and ordered structures than native or hydroxypropylated starches (Bahrami et al., 2024, Kittipongpatana et al., 2022). The form of dual-modified tigernut starch (SUD) fell between that of hydroxypropylated and cross-linked starches. Aggregation was present, but the granules still appeared pretty compact with little surface irregularity. The combined effect of hydroxypropylation and cross-linking balances granule flexibility with structural stability, creating starches with improved functional properties without compromising granule integrity. Similar results were observed for dual-modified cereal and tuber starches, in which hydroxypropylation increased granule flexibility, while phosphate cross-linking prevented excessive collapse of the structure (Rashwan et al., 2024).

The modified water yam starches (SMH, SMC, SMD, SRH, SRC, SRD) exhibited mainly oval to ellipsoidal granules, which agreed with the morphology generally reported for Dioscorea starches. The hydroxypropylated samples (SMH and SRH) showed granules with relatively smooth surfaces but with a greater tendency to aggregate than the native starches. The granule shape was maintained, indicating that the hydroxypropylation reaction occurred mainly in the amorphous regions, without significant damage to the granules. Similar retention of the granule form after hydroxypropylation was reported for yam and cassava starches (Tong et al., 2025).

Cross-linked water yam starches (SMC and SRC) showed greater granule aggregation and structural uniformity. The granules were less deformed and more resistant to surface erosion than the hydroxypropylated samples. This observation agrees with the role of phosphate cross-links in increasing intermolecular interactions in starch granules. STMP/STPP treatment has also been reported to improve the compactness and reduce the granule damage of cross-linked yam, sweet potato, and potato starches (Yan et al., 2025).

The dual-modified water yam starches (SMD and SRD) presented significant granule aggregation and dense packing, indicating the synergistic action of hydroxypropyl substitution and phosphate cross-linking. No significant granule breaking or collapse was observed, indicating that the two-step modification method did not substantially alter granule structure. Similar morphological stability was shown in dual-modified starches of cassava and sweet potato, where the combination of changes enhanced structural integrity without loss of granule identity (Rashwan et al., 2024).

The trifoliate yam starches (SNH, SNC and SND) had a significantly different shape compared to the water yam samples. The micrographs showed thick aggregates with rough surfaces and single grains that were marginally unclear. The hydroxypropylated sample (SNH) exhibited a sponge-like, porous structure indicative of partial disintegration of the starch matrix. The cross-linked sample (SNC) exhibited

increased density and consolidation, but the dual-modified starch (SND) had a highly aggregated structure with little evidence of granule fragmentation. The aggregation has been ascribed to the improvement of intermolecular contacts, as reported for chemically treated yam and legume starches (Yan et al., 2025).

Energy-Dispersive X-ray Spectroscopy

EDS analysis (Table 7) revealed that the primary elements in the modified starches were carbon and oxygen, confirming the carbohydrate-rich nature of the starch granules. Similar findings were observed in modified KJ CMU-107 rice starch, in which it was shown that the main elemental components were carbon and oxygen, but other elements such as sodium and phosphorus were found following chemical alteration (Kittipongpatana et al., 2022).

Phosphorus is found in several cross-linked and dual-modified starches, indicating the incorporation of phosphate groups from sodium trimetaphosphate and sodium tripolyphosphate. This is in agreement with studies that show the STMP/STPP cross-linking introduces phosphate bridges into the starch chains that may contribute to enhanced granular stiffness and functional stability (Rashwan et al., 2024). Yan et al. (2025) also discovered phosphorus in cross-linked starch using trimetaphosphate. Bahrami et al. (2024) investigated the signals of sodium and phosphorus in STMP-cross-linked potato starch and attributed them to effective phosphate modification.

The phosphorus levels in the present investigation were typically within the range expected for chemically phosphorylated starches, while differences between samples may be attributed to botanical source, reagent availability, granule size, washing efficiency, and the surface-sensitive nature of EDS. Phosphorus incorporation was more evident in the cross-linked and dual-modified samples than in hydroxypropylated starches. This is reasonable as hydroxypropylation largely introduced hydroxypropyl ether groups but not phosphate groups. Similar discrepancies between hydroxypropylated and cross-linked starches have been found in modified rice starch, where cross-linked starch had more P than hydroxypropyl starch (Kittipongpatana et al., 2022).

Sodium was also observed in several samples, especially in cross-linked starches. This may be due to leftover sodium salts from treatment with STMP/STPP. Similar Na signals have been reported for chemically treated starches and often indicate residues or counter-ions from the reagents; they are also associated with phosphate groups. However, because EDS is mostly sensitive to the sample surface, the Na content must be interpreted qualitatively and cannot be taken as a direct measure of overall starch substitution.

The EDS results confirmed efficient starch modification, specifically the incorporation of phosphate-containing groups in the cross-linked and dual-modified samples. FTIR and SEM findings, along with the co-presence of P and Na, further confirm that the chemical treatment changed the surface chemistry of the starch granules.

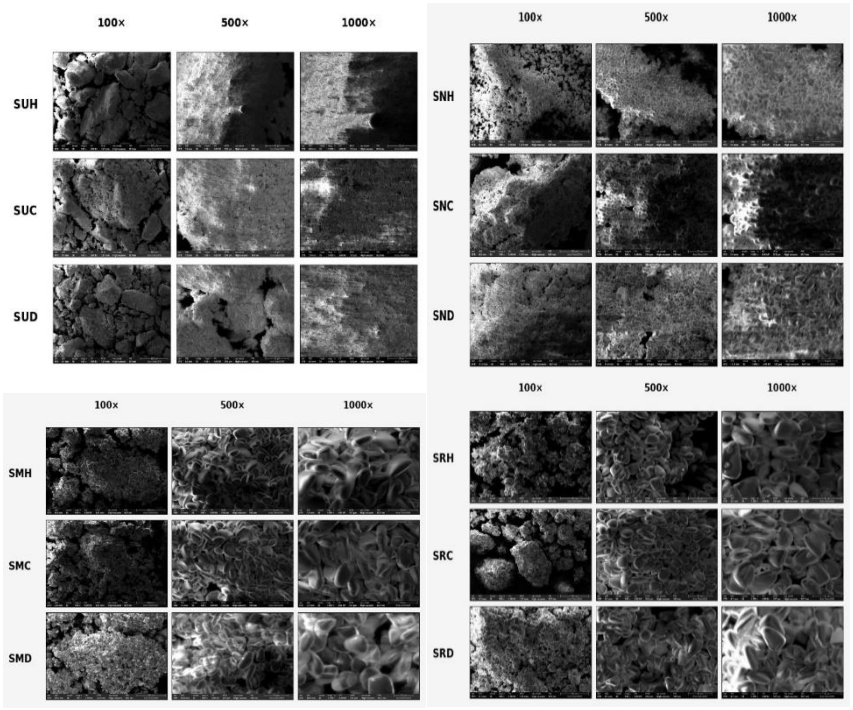


Figure 4: SEM micrographs of modified starches

Table 7: Surface Elemental Composition (%) of Modified Starches Determined by EDS

Source	Modification	C	O	Na	P
Tigernut	Hydroxypropylated	24.2	72.9	1.6	1.3
	Cross-linked	24.2	67.9	6.4	1.5
	Dual-modified	17.3	54.7	7.6	1.0
Trifoliate Yam	Hydroxypropylated	26.2	71.9	ND	1.9
	Cross-linked	24.5	70.9	3.9	0.7
	Dual-modified	23.2	75.8	ND	1.0

Source	Modification	C	O	Na	P
Water Yam I	Hydroxypropylated	25.1	74.9	ND	ND
	Cross-linked	24.8	73.5	1.7	ND
	Dual-modified	ND	100.0	ND	ND
Water Yam II	Hydroxypropylated	23.4	76.0	ND	0.6
	Cross-linked	24.0	71.0	3.4	1.6
	Dual-modified	22.9	75.7	ND	1.4

Fourier Transform Infrared (FTIR) Analysis

Table 8 and Figure 5 show FTIR spectra of hydroxypropylated, cross-linked, and dual-modified tigernut (SN), water yam cultivar I (SR), water yam cultivar II (SM), and trifoliate yam (SU) starches. All modified starches showed characteristic starch absorption bands, suggesting that the chemical alterations changed the molecular framework without destroying the basic polysaccharide backbone. The broad absorption band in the range of 3600–3200 cm^{-1} was assigned to the O–H stretching vibrations of hydroxyl groups and intermolecular hydrogen bonding. Small differences in band intensity for the modified starches reflect changes in hydrogen-bond interactions following hydroxypropylation and phosphate cross-linking. Kibar et al. (2024) reported similar observations for chemically modified starches. The band at 2920 cm^{-1} was assigned to C–H stretching vibrations of the glucose units. The presence of this band in all the modified starches indicated that the modification did not affect the glucopyranose framework. The band at about 1640 cm^{-1} was attributed to the bending vibration of adsorbed water, suggesting a variation in water association due to the structural modification. Among the modified starches, the most significant spectral changes were observed in the fingerprint region (1200-900 cm^{-1}). This area contains distinctive vibrations of C–O, C–O–C, and the glycosidic bond of starch. The small difference in band intensity in this area shows that chemical substitution was possible without disturbing the native starch framework. The absence of additional strong absorption bands further indicates that hydroxypropylation and phosphate cross-linking occurred at very modest degrees of substitution, which is common for food-grade modified starches (Singh et al., 2007). Generally, the dual-modified samples showed more pronounced changes in the fingerprint region than the hydroxypropylated and cross-linked starches individually, indicating a synergistic effect of hydroxypropyl substitution and phosphate cross-link formation on the molecular environment. Similar results have been seen in sequentially modified starches, where double modification yields greater changes in molecular organization than single modification (Gunaratne et al., 2007). Regarding the corrosion inhibition potential of the starch, the FTIR data showed that the modified starches contain numerous oxygen functional groups, such as hydroxyl, ether, and glycosidic oxygen atoms. These functional groups can serve as possible adsorption centers for lone-pair electron donation and hydrogen bonding with the metal surfaces, thereby forming a protective adsorbed coating. Additional phosphate functionalities supplied during cross-linking may further increase adsorption on the metal surface. Hydroxypropyl substitution promotes polymer hydration and dispersion. Therefore, FTIR analysis reveals that the modified starches have the structural characteristics required for efficient adsorption in corrosion inhibition.

Table 8: Characteristic FTIR Absorption Bands of the Modified Starches

Wavenumber (cm^{-1})	Functional group	Vibrational assignment	FTIR observation	Structural significance
3600–3200	O–H	Stretching vibration of hydroxyl groups	Broad absorption band observed in all hydroxypropylated, cross-linked, and dual-modified starches with slight variations in intensity.	Indicates abundant hydroxyl groups participating in intermolecular hydrogen bonding; intensity variations suggest modification-induced changes in hydrogen-bond interactions.
2930–2915	C–H	Asymmetric stretching of CH and CH_2 groups	Present in all modified starches with negligible spectral shifts.	Confirms that chemical modification did not alter the glucopyranose backbone of the starch molecules.
1655–1635	H–O–H	Bending vibration of absorbed water	Detected in all modified starches with minor differences in band intensity.	Reflects variations in moisture association arising from hydroxypropyl substitution and phosphate cross-link formation.
1450–1330	C–H / O–H	Bending and deformation vibrations	Slight intensity changes observed among the modification treatments.	Suggests localized alterations in the hydroxyl environment caused by the introduction of hydroxypropyl and phosphate functional groups.
1160–1145	C–O–C	Glycosidic bridge stretching vibration	Characteristic absorption band retained in all modified starches.	Demonstrates preservation of α-(1→4) glycosidic linkages and the integrity of the starch polysaccharide

Wavenumber (cm^{-1})	Functional group	Vibrational assignment	FTIR observation	Structural significance
				backbone following modification.
1085–1015	C–O	Stretching vibration of C–O bonds in glucose residues	Slight shifts and intensity variations observed across the modified starches.	Indicates successful chemical substitution while maintaining the fundamental starch molecular framework.
1022–995	Fingerprint region	Skeletal vibration of starch molecules	Greatest spectral variation is observed among hydroxypropylated, cross-linked, and dual-modified starches.	Reflects modification-induced changes in molecular organization, short-range crystallinity and structural ordering within the starch granules.

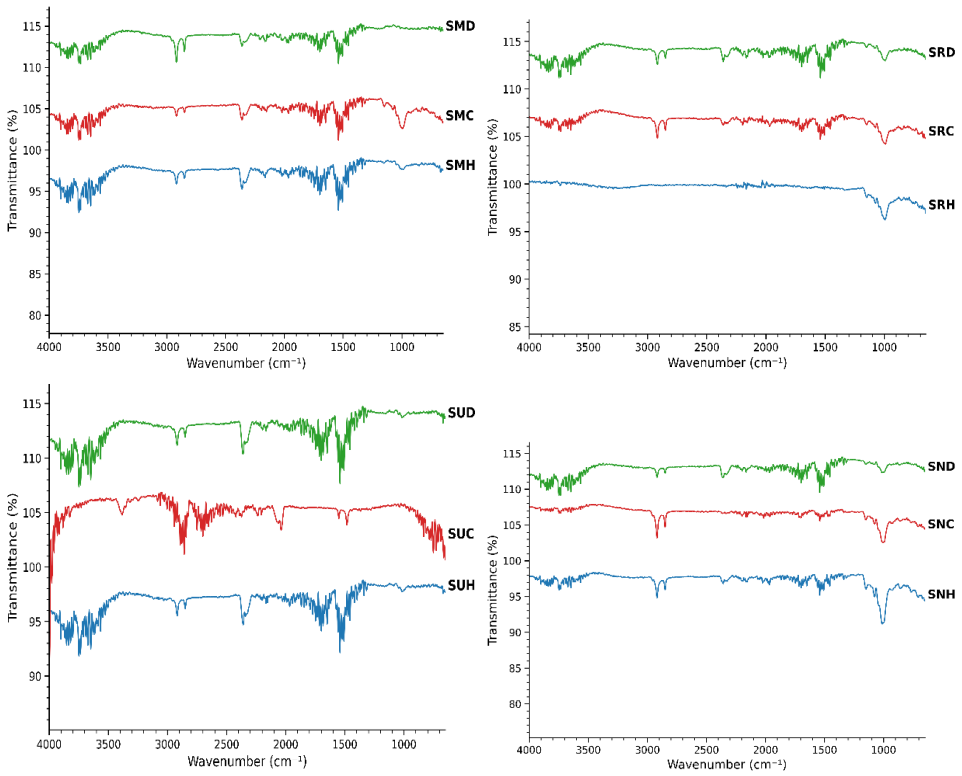


Figure 5: FTIR spectra of modified starches (SUH = Hydroxypropylated water yam starch, SUC = Cross-linked water yam starch, SUD = Dual-modified water yam starch, SMH = Hydroxypropylated water yam cultivar 2 starch, SMC = Cross-linked water yam cultivar 2 starch, SMD = Dual-modified water yam cultivar 2 starch, SRH = Hydroxypropylated trifoliate yam starch, SRC = Cross-linked trifoliate yam starch, SRD = Dual-modified trifoliate yam starch, SNH = ydroxypropylated tigernut starch, SNC = Cross-linked tigernut starch, SND = Dual-modified tigernut starch)

X-ray Diffraction Analysis

Figure 6 shows the X-ray diffraction patterns of hydroxypropylated, cross-linked, and dual-modified tigernut starches from water yam cultivars I and II, and trifoliate yam starches. The diffraction peaks of starch between 15–24° (2θ) were typical for all modified starches, indicating that the chemical alterations did not alter the fundamental crystalline polymorphs of the parent starches but did change their molecular organization. Similar observations have been reported for hydroxypropylated and cross-linked starches, where chemical alteration occurs mostly in the amorphous regions while keeping the crystalline structure of the granules (Kibar et al., 2024). Among the modified starches, hydroxypropylated starches often had larger and less defined diffraction peaks than cross-linked and dual-modified starches. Such behaviour indicates partial disruption of intermolecular hydrogen bonding and a decrease in the packing order of amylopectin double helices after hydroxypropyl substitution. Reductions in crystalline order following hydroxypropylation have been linked to the introduction of bulky hydroxypropyl groups that increase intermolecular spacing and molecular mobility (Singh et al., 2007). The diffraction peaks of the cross-linked and dual-modified starches were quite sharp, indicating that phosphate cross-linking improved structural integrity by restricting molecular mobility without sacrificing the native crystalline structure. A similar result was obtained for phosphate cross-linked starches, where covalent phosphate bridges stabilized the granular structure and preserved the normal starch diffraction pattern (Gunaratne et al., 2007). The much brighter reflections in the dually modified samples imply a balanced structural arrangement resulting from increased molecular flexibility and increased granule stability through sequential hydroxypropylation and cross-linking. The XRD

results indicated that the modification strategies significantly changed the supramolecular organization of the starches, maintaining their crystalline framework and producing structural features suitable for further evaluation as environmentally friendly corrosion inhibitors. The relative crystallinity (Crl) of the modified starches ranged from 23.1 to 33.9% (Table 9), indicating that hydroxypropylation, cross-linking, and dual modification altered the degree of molecular order without significantly disrupting the native crystalline structure. Dual-modified trifoliate yam starch (SUD) showed the highest crystallinity (33.9%), while several hydroxypropylated and aqueous yam starches showed lower values, suggesting partial disintegration of crystalline areas during chemical modification.

Table 9: Characteristic X-ray Diffraction Peaks, Crystal Type and Relative Crystallinity of Hydroxypropylated, Cross-Linked and Dual-Modified Starches from Selected Tropical Tuber Crops

Sample	Characteristic diffraction peaks (2θ, °)	Crystal type	Crl (%)
SNH	15.30, 17.52, 18.20, 23.24	A-type	24.8
SNC	15.38, 17.84, 18.18, 23.26	A-type	25.7
SND	15.10, 17.18, 18.54, 23.30	A-type	26.8
SUH	15.42, 17.19, 18.28, 23.52	A-type	25.0
SUC	15.44, 17.20, 18.46, 23.16	A-type	24.8
SUD	15.24, 17.32, 18.24, 23.64	A-type	33.9
SMH	5.80, 15.14, 17.20, 17.32, 19.72, 22.36, 23.84	C-type (B-dominant)	24.0
SMC	6.90, 15.58, 17.36, 19.68, 22.84, 23.26	C-type (B-dominant)	24.1
SMD	5.84, 15.12, 17.20, 19.74, 22.00, 23.74, 26.12	C-type (B-dominant)	23.1
SRH	5.76, 15.48, 17.48, 19.02, 22.84, 23.44, 24.06, 26.16	C-type (B-dominant)	24.0
SRC	5.88, 15.91, 17.33, 19.51, 22.36, 23.30, 24.42, 26.75	C-type (B-dominant)	24.4
SRD	5.81, 15.59, 17.38, 19.27, 22.57, 24.02, 26.32	C-type (B-dominant)	23.2

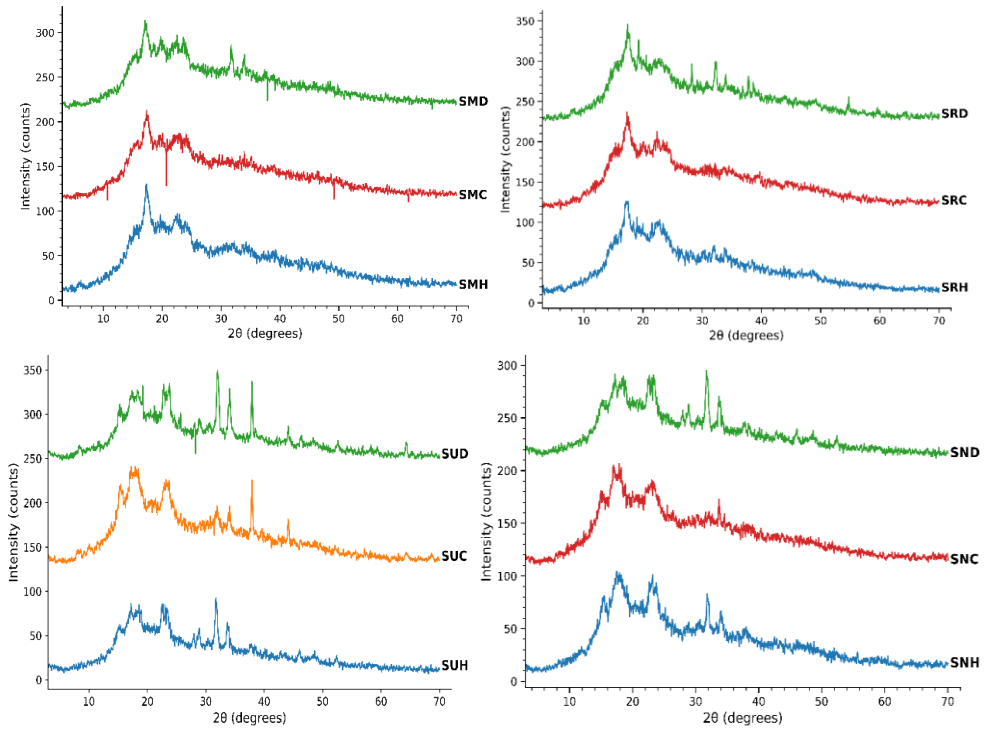


Figure 6: XRD patterns of modified starches

Pasting Characteristics of the Modified Starches

The plots from the RVA (Figure 7) and the pasting parameter properties (Table 10) suggested that the pasting behaviour of the modified starches was significantly affected by botanical root and modification method. Overall, the cross-linking modification technique yielded the highest maximum peak and hold viscosities. Cross-linked water yam cultivar II (SMC) achieved the lowest peak viscosity (607 cP), while hydroxypropylated trifoliate yam starch recorded the highest peak viscosity (3332 cP). The higher peak viscosity after cross-linking indicates better granule integrity and resistance to disintegration on heating. This was related to the formation of phosphate bridges, which enhanced intermolecular connections in starch granules. Similar benefits in the stability of modified starch paste with phosphate as a cross-linking agent for maize, cassava, and potato starches were reported by Gunaratne and Corke (2007) and Kibar et al. (2024). In contrast, hydroxypropylated starches typically exhibited lower peak and hold viscosities than their cross-linked counterparts. Hydroxypropyl groups interfere with intermolecular hydrogen bonding and introduce molecular flexibility, which favours granule expansion but decreases susceptibility to shear-induced disintegration upon heating. Similar decreases in viscosity after hydroxypropylation have been reported for cereal and tuber starches and have been attributed to increased molecular mobility and reduced

granular cohesion (Singh et al., 2007, Wang et al., 2020). The decreased viscosity of hydroxypropylated trifoliate yam starch further shows that the response to modification depends strongly on botanical origin and the starch's original molecular architecture. Dual modification led to an intermediate behaviour between hydroxypropylation and cross-linking, although the response varied among starch sources. For example, dual-modified water yam cultivar I (SRD) showed relatively high peak and hold viscosities, suggesting that phosphate cross-linking partially offset the reduction in structural integrity caused by hydroxypropyl substitution. This behaviour is consistent with previous reports that showed that sequential modification combines the enhanced hydration from hydroxypropylation and the enhanced thermal stability from cross-linking, resulting in starches with balanced functional properties (Singh et al., 2019, Ashogbon et al., 2014). In particular, the increased paste stability of the cross-linked and dual-modified starches is important given their applicability as green corrosion inhibitors. More structurally stable starches should yield more cohesive polymeric films that can withstand surface coverage in harsh conditions. Hydroxypropyl substitution will promote hydration and dispersion in aqueous media. Together, these structural features may promote adsorption of hydroxyl-, ether-, and phosphate-containing polymer chains onto the metal surface, fostering a stable protective barrier against corrosive substances. Similar relationships between the polysaccharide structure and corrosion inhibition have been reported for starch-based inhibitors in acid media (Lahrour et al., 2019, Quadri et al., 2023). Thus, the RVA results revealed the advantageous combination of dispersibility and structural stability of the dual-modified starches, particularly the water yam starches, which may improve their performance as environmentally benign corrosion inhibitors.

Table 10: Pasting Properties of Hydroxypropylated, Cross-Linked, and Dual-Modified Starches from Four Botanical Sources

Source	Sample	Peak viscosity (PV, cP)	Trough viscosity (TV, cP)	Breakdown (BDV, cP)	Final viscosity (FV, cP)	Setback (SBV, cP)	Peak time (min)	Pasting temp. (°C)
Water yam I	SMH	2539 ± 1.00^{c}	2026 ± 1.00^{c}	513 ± 0.00^{b}	3735 ± 1.00^{c}	1709 ± 0.00^{b}	5.27 ± 0.02^{b}	83.2 ± 0.02^{c}
	SMC	3392 ± 1.00^{a}	2805 ± 1.00^{a}	587 ± 0.00^{a}	5020 ± 1.00^{a}	2215 ± 0.00^{a}	5.20 ± 0.01^{c}	84.2 ± 0.02^{b}
	SMD	2778 ± 1.53^{b}	2471 ± 1.53^{b}	307 ± 0.00^{c}	4154 ± 1.53^{b}	1683 ± 0.00^{c}	5.67 ± 0.02^{a}	85.8 ± 0.10^{a}
Water yam II	SRH	2238 ± 0.58^{c}	1815 ± 0.58^{c}	423 ± 0.00^{c}	2944 ± 0.58^{c}	1129 ± 0.00^{c}	5.43 ± 0.02^{b}	84.1 ± 0.02^{a}
	SRC	3162 ± 1.00^{a}	2719 ± 1.00^{a}	443 ± 0.00^{b}	4907 ± 1.00^{a}	2188 ± 0.00^{a}	5.33 ± 0.01^{c}	83.3 ± 0.10^{b}
	SRD	2874 ± 1.00^{b}	2429 ± 1.00^{b}	445 ± 0.00^{a}	3944 ± 1.00^{b}	1515 ± 0.00^{b}	5.53 ± 0.02^{a}	84.1 ± 0.02^{a}
Trifoliate yam	SUH	607 ± 0.58^{c}	271 ± 0.58^{c}	336 ± 0.00^{c}	379 ± 0.58^{c}	108 ± 0.00^{c}	4.82 ± 0.02^{c}	88.1 ± 0.02^{b}
	SUC	1713 ± 0.58^{b}	1159 ± 0.58^{b}	554 ± 0.00^{b}	1552 ± 0.58^{a}	393 ± 0.00^{a}	5.00 ± 0.02^{b}	88.1 ± 0.02^{b}
	SUD	1751 ± 0.58^{a}	1182 ± 0.58^{a}	569 ± 0.00^{a}	1516 ± 0.58^{b}	334 ± 0.00^{b}	5.27 ± 0.02^{a}	90.5 ± 0.02^{a}
Tigernut	SNH	2181 ± 0.58^{c}	1444 ± 0.58^{c}	737 ± 0.00^{b}	2453 ± 0.58^{c}	1009 ± 0.00^{c}	4.73 ± 0.02^{a}	83.2 ± 0.02^{a}
	SNC	2689 ± 0.58^{a}	1919 ± 0.58^{a}	770 ± 0.00^{a}	3091 ± 0.58^{b}	1172 ± 0.00^{b}	4.67 ± 0.02^{b}	80.9 ± 0.03^{c}
	SND	2372 ± 1.00^{b}	1726 ± 1.00^{b}	646 ± 0.00^{c}	3185 ± 1.00^{a}	1459 ± 0.00^{a}	4.73 ± 0.02^{a}	81.6 ± 0.02^{b}

Abbreviations: PV, peak viscosity; TV, trough viscosity; BDV, breakdown viscosity; FV, final viscosity; SBV, setback viscosity; PKT, peak time; PT, pasting temperature. Values are presented as mean ± standard deviation (n = 3). Means within a column followed by different superscript letters differ significantly (Tukey's HSD test, $p < 0.05$).

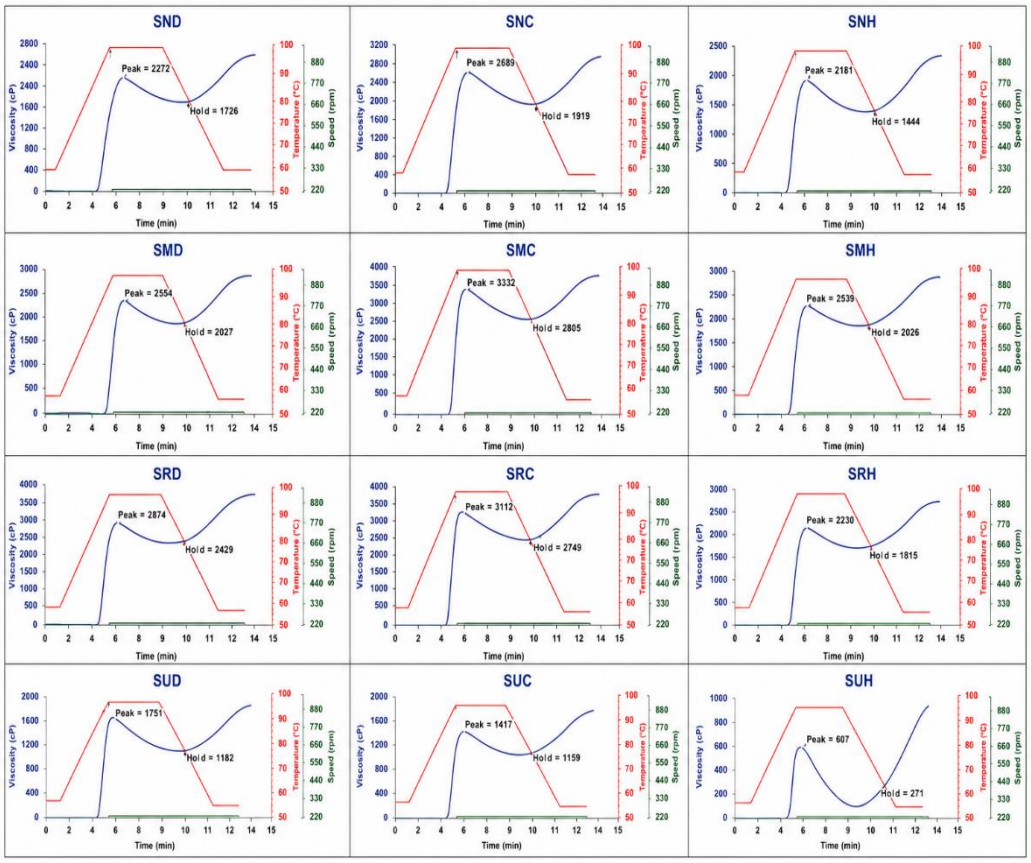


Figure 7: RVA plots of modified starches

Thermal Properties of Modified Starches

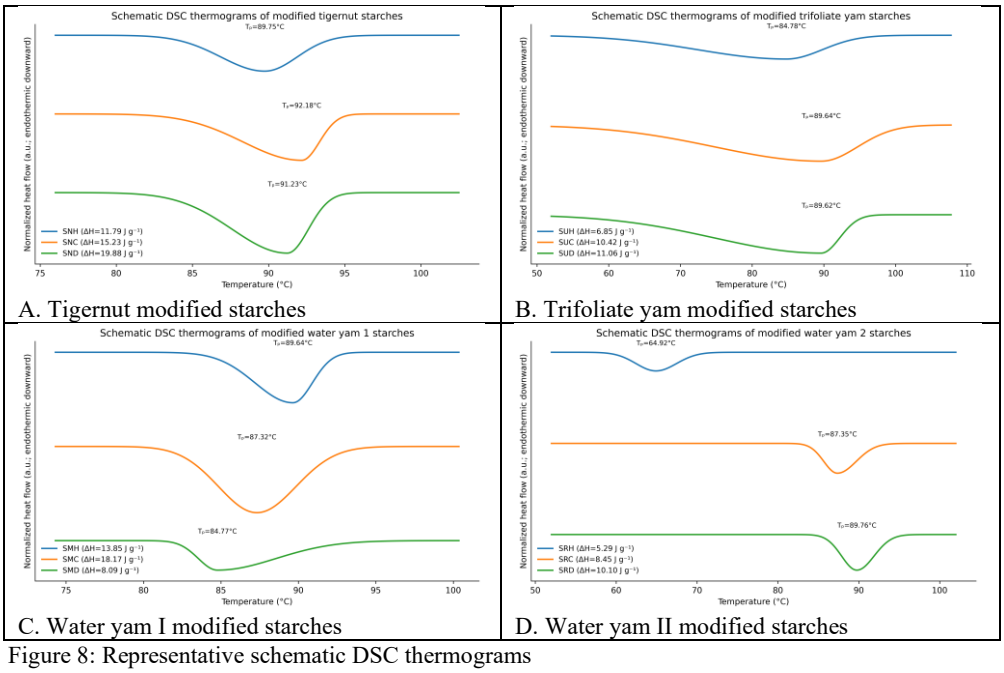
Table 11 and Figure 8 show the differential scanning calorimetry parameters of modified starches. The DSC measurements show a strong source-dependent response to the chemical alteration. Factorial ANOVA indicated significant impacts of botanical source, modification type, and their interaction on all four thermal indices ($p < 0.001$). This interaction is scientifically relevant because it reveals that the direction and extent of the modification reaction depend on the native molecular and supramolecular architecture of each starch. The botanical origin dictates amylose/amylopectin organization, crystalline polymorph, granule morphology, and reagent accessibility; therefore, identical modification conditions may produce different thermal reactions across starches (Núñez-Bretónet al., 2026, Kumari et al., 2023). The changes led to a consistently high gelatinization temperature range of tigernut starch. The highest peak temperature was observed for cross-linking (92.18 °C), hydroxypropylation (89.75 °C), and dual modification (91.23 °C). The increased T_p for the cross-linked sample is consistent with the formation of covalent phosphate bridges that strengthen inter-chain connections, restrict chain mobility, and require more thermal energy before crystalline regions melt. Similarly, recent studies report cross-linking as a method to reinforce the granular structure and boost resistance to heat, shear, and acidic processing conditions (Punia Bangar et al., 2024). However, the dual modified starch had the highest tigernut enthalpy (19.88 J g^{-1}), showing that the sequential treatment produced a more energetically intensive ordered domain compared to any of the single treatments. This non-additive response is consistent with the idea that dual modification can cause structural reorganization, rather than just summing the effects of the two individual reactions (Núñez-Bretónet al., 2026). In trifoliate yam starch, T_o remained essentially unchanged at approximately 60 °C across the three treatments, but T_p increased from 84.78 °C in the hydroxypropylated sample to approximately 89.6 °C in the cross-linked and dual-modified samples. Hydroxypropylation also produced the lowest ΔH (6.85 J g^{-1}), whereas cross-linking and dual modification increased ΔH to 10.42 and 11.06 J g^{-1}, respectively. Hydroxypropyl groups disrupt inter- and intramolecular hydrogen bonding, enhance water penetration, and weaken ordered double-helical regions, commonly lowering the energy required for gelatinization. Paramitasari et al. (2024) likewise reported reductions in gelatinization temperature and enthalpy following hydroxypropylation of sago starch (Paramitasari et al., 2024). The higher values after cross-linking indicate granule reinforcement and reduced molecular mobility. Water yam 1 displayed a different response. Hydroxypropylation produced the highest T_o and T_p (84.76 and 89.64 °C), while dual modification markedly reduced T_p to 84.77 °C and ΔH to 8.09 J g^{-1}. In contrast, cross-linking generated the highest ΔH (18.17 J g^{-1}). This suggests that phosphate cross-links stabilized pre-existing ordered structures, whereas the combined treatment disrupted or redistributed a substantial proportion of the crystallite population despite retaining a relatively high onset temperature. The reduced enthalpy of the dual-modified sample implies fewer or less perfect double helices available for cooperative melting. Such non-linear outcomes are increasingly recognized in multiply modified starches, where treatment sequence, substitution level, and source structure determine whether the final response is synergistic, antagonistic, or merely additive (Núñez-Bretónet al., 2026). Water yam 2 showed the widest modification-dependent shift. Hydroxypropylation yielded much lower T_o, T_p, and T_c

values (60.00, 64.92, and 70.00 °C) and the lowest ΔH (5.29 J g^{-1}), indicating substantial weakening of crystalline and double-helical order and easier water-assisted gelatinization. Cross-linking increased these values to 84.00, 87.35, and 92.00 °C, while dual modification produced the highest transition temperatures (86.00, 89.76, and 94.00 °C) and a higher enthalpy (10.10 J g^{-1}). The hydroxypropylated pattern agrees with current evidence that hydroxypropyl substitution increases chain spacing and hydrophilicity while reducing the energy required for gelatinization (Kibar et al., 2024). Conversely, the dual-modified water yam 2 appears to have retained the flexibility introduced by hydroxypropyl groups while acquiring a reinforced network through cross-linking. From an application perspective, samples with higher T_p and T_c, particularly cross-linked tigernut and dual-modified water yam 2, should tolerate higher processing temperatures before complete gelatinization and may suit applications requiring thermal and shear stability. Hydroxypropylated water yam 2, with its low transition temperatures and low ΔH, may be advantageous in systems requiring rapid cooking, reduced thermal input, or easy hydration. High ΔH values, such as those of dual-modified tigernut and cross-linked water yam 1, indicate a greater energy requirement to disrupt ordered structures and may correspond to more thermally resistant granular organization.

Table 11: Differential Scanning Calorimetry Parameters of Modified Starches

Starch source	Modification	Code	T_o (°C)	T_p (°C)	T_c (°C)	ΔH (J g^{-1})
Tigernut	Hydroxypropylated	SNH	84.00 ± 0.10^{b}	89.75 ± 0.05^{c}	94.00 ± 0.02^{d}	11.79 ± 0.01^{e}
	Cross-linked	SNC	84.50 ± 0.10^{b}	92.18 ± 0.02^{a}	94.50 ± 0.02^{c}	15.23 ± 0.01^{c}
	Dual-modified	SND	84.00 ± 1.00^{b}	91.23 ± 0.01^{b}	94.00 ± 0.01^{d}	19.88 ± 0.01^{a}
Trifoliate yam	Hydroxypropylated	SUH	60.00 ± 0.01^{d}	84.78 ± 0.02^{f}	94.80 ± 0.02^{b}	6.85 ± 0.02^{k}
	Cross-linked	SUC	59.98 ± 0.02^{d}	89.64 ± 0.02^{d}	99.74 ± 0.02^{a}	10.42 ± 0.02^{g}
	Dual-modified	SUD	59.98 ± 0.02^{d}	89.62 ± 0.02^{d}	94.77 ± 0.02^{b}	11.06 ± 0.02^{f}
Water yam 1	Hydroxypropylated	SMH	84.76 ± 0.02^{b}	89.64 ± 0.02^{d}	92.16 ± 0.02^{f}	13.85 ± 0.02^{d}
	Cross-linked	SMC	82.37 ± 0.02^{c}	87.32 ± 0.02^{e}	92.36 ± 0.05^{e}	18.17 ± 0.02^{b}
	Dual-modified	SMD	82.31 ± 0.02^{c}	84.77 ± 0.02^{f}	92.33 ± 0.02^{e}	8.09 ± 0.02^{j}
Water yam 2	Hydroxypropylated	SRH	60.00 ± 0.02^{d}	64.92 ± 0.02^{g}	70.00 ± 0.02^{h}	5.29 ± 0.03^{l}
	Cross-linked	SRC	84.00 ± 0.03^{b}	87.35 ± 0.02^{e}	92.00 ± 0.03^{g}	8.45 ± 0.02^{i}
	Dual-modified	SRD	86.00 ± 0.02^{a}	89.76 ± 0.02^{c}	94.00 ± 0.02^{d}	10.10 ± 0.02^{h}

Values are means ± SD (n = 3). Within each column, means bearing different superscript letters differ significantly (Tukey's HSD, $p < 0.05$). T_o, onset temperature; T_p, peak temperature; T_c, conclusion temperature; ΔH, gelatinization enthalpy. H, hydroxypropylated; C, cross-linked; D, dual-modified.



A. Tigernut modified starches

B. Trifoliate yam modified starches

C. Water yam I modified starches

D. Water yam II modified starches

Figure 8: Representative schematic DSC thermograms

Hydroxypropyl and Phosphate Substitution Characteristics of Modified Starches

Table 12 presents the hydroxypropyl group content (HGC), molar substitution (MS), phosphorus content (PC), and phosphate degree of substitution (DS) of the modified starches. These parameters provide quantitative evidence of chemical substitution and offer insight into modification-induced differences in starch structure and functionality. The extent of substitution varied with botanical origin and modification treatment, reflecting possible differences in hydroxyl-group accessibility and granular organization. Singly hydroxypropylated starches showed HGC values of 1.28–1.81%, corresponding to MS values of 0.036–0.051. Hydroxypropylated water yam variety 2 (SRH) recorded the highest HGC (1.81%; MS = 0.051), whereas trifoliate yam (SUH) exhibited the lowest (1.28%; MS = 0.036). Following

dual modification, HGC increased to 1.53–2.06%, with corresponding MS values of 0.043–0.059. The highest substitution was observed in dual-modified water yam variety 2 (SRD; HGC = 2.06%, MS = 0.059). However, the effect of sequential modification was source-dependent, as HGC increased in tigernut and water yam variety 2 but decreased slightly in water yam variety 1. These variations suggest that the extent of hydroxypropyl incorporation was influenced by the botanical characteristics of the starches and the modification conditions. Similar source-dependent responses have been reported for chemically modified starches (Wattanachantet al., 2003, Fu et al., 2019).

The cross-linked starches exhibited phosphorus contents of 0.088–0.142%, corresponding to phosphate DS values of 0.0046–0.0075. Cross-linked water yam variety 2 (SRC) recorded the highest phosphorus incorporation (0.142%; DS = 0.0075), while cross-linked trifoliate yam (SUC) exhibited the lowest (0.088%; DS = 0.0046). In the dual-modified starches, phosphorus content ranged from 0.060 to 0.113%, with corresponding DS values of 0.0031–0.0059. Dual-modified tigernut starch (SND) exhibited the highest phosphorus content (0.113%; DS = 0.0059). Compared with their corresponding singly cross-linked starches, phosphorus incorporation increased slightly in tigernut and trifoliate yam but decreased in both water yam varieties. This indicates that sequential hydroxypropylation and phosphate treatment did not uniformly enhance phosphorus incorporation, possibly because of differences in reactive-site accessibility and molecular organization (Wattanachantet al., 2003 , Ashogbon, 2021).

Table 12: Hydroxypropyl and Phosphate Substitution Characteristics of Chemically Modified Starches

Sample	HGC (%)	MS	PC (%)	DS
SNH	1.40	0.040	—	—
SNC	—	—	0.106	0.0056
SND	1.95	0.056	0.113	0.0059
SUH	1.28	0.036	—	—
SUC	—	—	0.088	0.0046
SUD	1.53	0.043	0.089	0.0047
SMH	1.80	0.051	—	—
SMC	—	—	0.105	0.0055
SMD	1.68	0.048	0.077	0.0040
SRH	1.81	0.051	—	—
SRC	—	—	0.142	0.0075
SRD	2.06	0.059	0.060	0.0031

HGC, hydroxypropyl group content; MS, molar substitution; PC, phosphorus content; DS, phosphate degree of substitution; —, not applicable.

Conclusion

Chemical modification of tigernut, water yam, and trifoliate yam starches through hydroxypropylation, phosphate cross-linking, and sequential dual modification significantly influenced their physicochemical, functional, structural, thermal, and pasting properties. The modification treatments altered moisture content, apparent amylose content, hydration behaviour, molecular organization, granule morphology, and viscosity characteristics while largely preserving the fundamental polysaccharide structure. FTIR analysis revealed modification-associated changes in functional-group environments, while EDS detected phosphorus in phosphate-treated starches. XRD analysis demonstrated retention of the characteristic crystalline polymorphs, with variations in relative crystallinity indicating changes in molecular ordering. SEM observations further revealed modification-dependent differences in granule morphology and aggregation. Hydroxypropylation generally enhanced hydration-related properties, whereas phosphate cross-linking restricted granule swelling and influenced paste stability. Sequential dual modification produced distinct responses depending on the botanical source, highlighting the importance of starch origin and treatment strategy in determining functional performance. The findings show that chemical modification effectively tailors the structure and functionality of underutilized tropical starches, establishing useful structure–property relationships for potential industrial applications. Further investigations involving electrochemical, gravimetric, and surface-characterization techniques are required to establish their suitability as sustainable corrosion inhibitors for mild steel.

Acknowledgement

The authors appreciate the management of Afe Babalola University, Ado Ekiti, Nigeria, for their support.

REFERENCES

Ashmawy, A.M. and M. Mostfa, *Study of eco-friendly corrosion inhibition for mild steel in acidic environment.* Egyptian Journal of Chemistry, 2021. 64(3): p. 1285-1291.

El-Housseiny, S., et al., *Eco-friendly corrosion inhibitor for mild steel in acidic media.* Int. J. Corros. Scale Inhib, 2022. 11(4): p. 1516-1538.

Furtado, L.B. and R. Nascimento, *Plant extracts as green corrosion inhibitors*, in *Sustainable corrosion inhibitors II: synthesis, design, and practical applications*. 2021, ACS Publications. p. 19-77.

Ahmed, M.A., S. Amin, and A.A. Mohamed, *Current and emerging trends of inorganic, organic and eco-friendly corrosion inhibitors.* RSC advances, 2024. 14(43): p. 31877-31920.

Verma, C., et al., *Principles and theories of green chemistry for corrosion science and engineering: design and application.* Green Chemistry, 2024. 26(8): p. 4270-4357.

Salim, A., et al., *Environmentally friendly green inhibitors used for corrosion inhibition of oil pipeline.* Int. J. Corros. Scale Inhib, 2026. 15(3): p. 27-57.

Gamage, A., et al., *Environmental properties and applications of biodegradable starch-based nanocomposites.* Polymers, 2022. 14(21): p. 4578.

Korniy, S., et al., *Eco-friendly metal corrosion inhibitors based on natural polymers (A review).* Materials Science, 2023. 58(5): p. 567-578.

Awoyale, R.B., et al., *Harnessing the Industrial Potential of Starch Derived From Selected Tuber Crops for the Pharmaceutical Industry: A Review.* Starch-Stärke, 2026. 78(1): p. e70151.

He, R., et al., *Starch modification with molecular transformation, physicochemical characteristics, and industrial usability: A state-of-the-art review.* Polymers, 2023. 15(13): p. 2935.

Amaraweera, S.M., et al., *Development of starch-based materials using current modification techniques and their applications: A review.* Molecules, 2021. 26(22): p. 6880.

Wang, H., et al., *Functional and physicochemical properties of flours and starches from different tuber crops.* International journal of biological macromolecules, 2020. 148: p. 324-332.

Ogunbiyi, B.I., S. Akano, and M.B. Yahaya, *PHYSICAL, CHEMICAL AND FUNCTIONAL PROPERTIES OF FLOUR AND STARCH FROM TWO TIGERNUT (Cyperus esculentus) VARIETIES.* FUDMA JOURNAL OF SCIENCES, 2026. 10(4): p. 148-154.

Wu, Y., et al., *Tiger nut (Cyperus esculentus) starch: extraction, composition, structure, properties, modification and uses.* Sustainable Food Technology, 2024. 2(3): p. 635-651.

Azima, F., N. Nazir, and H. Efendi. *Characteristics of physico-chemical and functional properties of starch extracts from tubers*. in *Journal of Physics: Conference Series*. 2020. IOP Publishing.

Talha, M., *Biomacromolecules as green corrosion inhibitors: a review based on mild steel corrosion in acidic media.* Corrosion Reviews, 2025. 43(4): p. 409-428.

Awoyale, R.B., et al., *Comparative Structural and Functional Characterization of Underutilized Tropical Tuber Starches: Implications for Pharmaceutical Excipient Development.* Starch-Stärke, 2026. 78(10): p. e70311.

Ishiwu, C., et al., *Physiochemical properties of cocoyam starch extracted in two media.* International Letters of Natural Sciences, 2017. 64.

Olatidoye, O., D. Adenoye, and B. Idemudia, *Influence of chemical modification on some properties of starches from tiger nut (Cyperus esculentus) and cocoyam (Xanthosoma sagittifolium) as a potential biomaterial.* Int. Res. J. Biol. Sci, 2019. 1: p. 13-24.

Woggum, T., P. Sirivongpaisal, and T. Wittaya, *Characteristics and properties of hydroxypropylated rice starch based biodegradable films.* Food Hydrocolloids, 2015. 50: p. 54-64.

Lawal, O.S., *Composition, physicochemical properties and retrogradation characteristics of native, oxidised, acetylated and acid-thinned new cocoyam (Xanthosoma sagittifolium) starch.* Food chemistry, 2004. 87(2): p. 205-218.

Gunaratne, A., S. Ranaweera, and H. Corke, *Thermal, pasting, and gelling properties of wheat and potato starches in the presence of sucrose, glucose, glycerol, and hydroxypropyl β-cyclodextrin.* Carbohydrate polymers, 2007. 70(1): p. 112-122.

Chandra, S., S. Singh, and D. Kumari, *Evaluation of functional properties of composite flours and sensorial attributes of composite flour biscuits.* Journal of food science and technology, 2015. 52(6): p. 3681-3688.

Xiang, G., et al., *The influence of temperature changes on the rice starch structure and digestive characteristics: One and two-step annealing.* Foods, 2022. 11(22): p. 3641.

Karmakar, B., R. Chakraborty, and S. Roy, *Assessment of yield and characterization of starch extracted using different methods from the corms of some aroids in North Bengal region of India.* Discover Food, 2025. 5(1): p. 290.

Okekunle, M.O., et al., *Physicochemical, morphological and thermal properties of oxidized starches from Lima bean (Phaseolus lunatus).* Scientific African, 2020. 8: p. e00432.

Amoo, A.R.N., W.-M.F. Dufie, and O. Ibok, *Physicochemical and pasting properties of starch extracted from four yam varieties.* Journal of Food and Nutrition Sciences, 2014. 2(6): p. 262-269.

Yadav, S., et al., *Characterisation of finger millet (Eleusine coracana) starch isolated by conventional and ultrasound-assisted starch isolation methods.* International Journal of Food Science and Technology, 2024. 59(8): p. 5710-5720.

Olayinka, F., et al., *Effect of chemical modifications on thermal, rheological and morphological properties of yellow sorghum starch.* Journal of food science and technology, 2015. 52(12): p. 8364-8370.

Punia Bangar, S., et al., *Recent advancements in cross-linked starches for food applications-a review.* International journal of food properties, 2024. 27(1): p. 411-430.

Kibar, E.A.A., et al., *Determination of Physicochemical and Functional Properties of Cross-Linked, Hydroxypropylated, and Dual Modified Corn Starch and Investigation of Its Use as Gelling Agent in Soft Confectionery.* Starch-Stärke, 2024. 76(7-8): p. 2300036.

Lagunes-Delgado, C., E. Agama-Acevedo, and L.A. Bello-Pérez, *Dual starch modifications to expand its end-uses: A review.* Starch-Stärke, 2024. 76(11-12): p. 2300153.

Mehfooz, T., et al., *Characterization of hydroxypropylated-distarch phosphate barley starch and its impact on rheological and sensory properties of soup.* International journal of biological macromolecules, 2020. 144: p. 410-418.

Chen, P., et al., *Comparison of the structure and properties of hydroxypropylated acid-hydrolysed maize starches with different amylose/amylopectin contents.* Food Hydrocolloids, 2021. 110: p. 106134.

Chandak, A., et al., *Effects of cross-linking on physicochemical and film properties of lotus (Nelumbo nucifera G.) Seed Starch.* Foods, 2022. 11(19): p. 3069.

Mehfooz, T., et al., *Morphological, functional and thermal characteristics of hydroxypropylated-crosslinked barley starches.* Journal of Food Measurement and Characterization, 2021. 15(1): p. 237-246.

Deng, S., X. Li, and G. Du, *An efficient corrosion inhibitor of cassava starch graft copolymer for aluminum in phosphoric acid.* Chinese Journal of Chemical Engineering, 2021. 37: p. 222-231.

Chen, M., et al., *An investigation of modified dialdehyde starch as a highly efficient green corrosion inhibitor for carbon steel in 1 M HCl medium: Synthesis, experimental and theoretical studies.* Industrial Crops and Products, 2024. 215: p. 118534.

Fu, Z., et al., *Developments in hydroxypropylation of starch: A review.* Starch-Stärke, 2019. 71(1-2): p. 1800167.

Park, M.H. and M. Kim, *Physicochemical properties of hydroxypropylated apios starches.* Preventive Nutrition and Food Science, 2020. 25(3): p. 286.

Kumar, Y., S. Singh, and D. Saxena, *A comprehensive review on methods, mechanisms, properties, and emerging applications of crosslinked starches.* International Journal of Biological Macromolecules, 2025. 306: p. 141526.

Zhang, R.-Y., et al., *Effects of different isolation methods on the structure and functional properties of starch from tiger nut (Cyperus esculentus L.) meal.* LWT, 2024. 196: p. 115853.

Bahrami, M., et al., *Cross-linked starch as media for crystal Violet elimination from water: modeling batch adsorption with fuzzy regression.* Molecules, 2024. 29(16): p. 3894.

Kittipongpatana, O.S. and N. Kittipongpatana, *Physicochemical and functional properties of modified KJ CMU-107 rice starches as pharmaceutical excipients.* Polymers, 2022. 14(7): p. 1298.

Rashwan, A.K., et al., *Plant starch extraction, modification, and green applications: A review.* Environmental Chemistry Letters, 2024. 22(5): p. 2483-2530.

Tong, C., et al., *Toward an understanding of potato starch structure, function, biosynthesis, and applications.* Food Frontiers, 2023. 4(3): p. 980-1000.

Yan, X., et al., *Characterisation of starch nanoparticles prepared by cross-linking and nanoprecipitation.* International Journal of Food Science and Technology, 2025. 60(2): p. vvaf025.

Singh, J., L. Kaur, and O. McCarthy, *Factors influencing the physico-chemical, morphological, thermal and rheological properties of some chemically modified starches for food applications—A review.* Food hydrocolloids, 2007. 21(1): p. 1-22.

Arawande, J.O. and A.O. Ashogbon, *Isolation and characterization of starch obtained from cocoyam cultivated at Akungba Akoko, Ondo State, Nigeria.* Nutri. and Food Sci. Int. J, 2019. 8(2): p. 1-6.

Ashogbon, A.O. and E.T. Akintayo, *Recent trend in the physical and chemical modification of starches from different botanical sources: A review.* Starch-Stärke, 2014. 66(1-2): p. 41-57.

Lahrour, S., et al., *Glycerin-grafted starch as corrosion inhibitor of C-Mn steel in 1 M HCl solution.* Applied Sciences, 2019. 9(21): p. 4684.

Quadri, T.W., et al., *Grafted Starch Used as Sustainable Corrosion Inhibitors.* Grafted Biopolymers as Corrosion Inhibitors: Safety, Sustainability, and Efficiency, 2023: p. 313-335.

Núñez-Bretón, L.C., et al., *Recent developments of multiple functionalization of starches: A review of physical, chemical, and enzymatic modifications and their industrial applications.* Journal of Food Measurement and Characterization, 2026. 20(6): p. 9527-9555.

Kumari, B. and N. Sit, *Comprehensive review on single and dual modification of starch: Methods, properties and applications.* International Journal of Biological Macromolecules, 2023. 253: p. 126952.

Paramitasari, D., et al., *Hydroxypropylation for functional enhancement of sago starch: The effects of low propylene oxide concentration using response surface methodology.* Journal of Agriculture and Food Research, 2024. 15: p. 100933.

Wattanachant, S., et al., *Effect of crosslinking reagents and hydroxypropylation levels on dual-modified sago starch properties.* Food Chemistry, 2003. 80(4): p. 463-471.

Ashogbon, A.O., *Dual modification of various starches: Synthesis, properties and applications.* Food chemistry, 2021. 342: p. 128325.

©2026 This is an Open Access article distributed under the terms of the Creative Commons Attribution 4.0 International license viewed via https://creativecommons.org/licenses/by/4.0/ which permits unrestricted use, distribution, and reproduction in any medium, provided the original work is cited appropriately.